NIC Symposium 2016

11 – 12 February 2016
Forschungszentrum Jülich, Germany

Programme

Bus Schedule

Poster Abstracts

Participants

Programme

Thursday, 11 February 2016

8:30	Transfer from Jülich
9:00	Registration
9:30	**Welcome Address** by W. Marquardt, Chairman of the Board of Directors, Forschungszentrum Jülich
9:45	Th. Lippert, Forschungszentrum Jülich **Scientific Big Data Analytics by HPC**
10:30	Coffee
11:00	M. Müser, Forschungszentrum Jülich **Percolation and the Physics of Seals**
11:45	P. Romero, Frauenhofer IWM **Understanding Tribology and Machining Processes through Computationally Intensive Large Scale MD**
12:30	Group Photograph
12:45	Lunch
14:00	K. Albe, TU Darmstadt **Nanostructured Metallic Glasses: Tayloring the Mechanical Properties of Amorphous Metals**
14:45	P. Nielaba, Universität Konstanz **Structures and Phases in (Nano-)Systems in Confined Geometry**
15:30	Coffee
16:00	P. Coto, Universität Erlangen-Nürnberg **Electron Transfer and Transport Processes at Molecule-Metal and Molecule-Semiconductor Interfaces**
16:45	G. Rossetti, Forschungszentrum Jülich **Intrinsic Disordered Protein in Diseases: A Computational Challenge**
17:30	**Poster Session and Reception**
19:00	Transfer to Jülich

Friday, 12 February 2016

8:30	Transfer from Jülich
9:00	M. Hoeft, Thüringer Landessternwarte Tautenberg **LOFAR: Calibration and Imaging on JURECA**
9:45	D. Seifried, Universität Köln **Interstellar Turbulence and Its Effects on the Formation of Protostellar Discs**
10:30	Coffee
11:00	C. Hölbling, Universität Wuppertal ***Ab Initio* Determination of the Neutron-Proton Mass Difference**
11:45	A. Schwenk, TU Darmstadt **The Strong Interaction at Neutron-Rich Extremes**
12:30	Lunch
14:00	R. Grauer, Universität Bochum **Dynamos, Reconnection and Turbulence**
14:45	I. Dornmair, Universität Hamburg **Towards Plasma-Driven Free-Electron Lasers**
15:30	Coffee
16:00	F. Leroy, TU Darmstadt **Multiscale Simulations of Solid-Liquid Interfaces**
16:45	H.Köstler, Universität Erlangen-Nürnberg **Massively Parallel Large Scale Stokes Flow Simulation**
17:30	End of NIC Symposium
17:45	Transfers to Jülich and to Düren Train Station

Bus Schedule

Bus is free of charge for participants.

Date	Departure Time	Meeting Point	Destination
11 February	08:30	Bus stop "Walramplatz"	Forschungszentrum Jülich, Auditorium
	08:35	Bus stop "Neues Rathaus"	
	19:00	Forschungszentrum Jülich, Auditorium	Hotels in Jülich
12 February	08:30	Bus stop "Walramplatz"	Forschungszentrum Jülich, Auditorium
	08:35	Bus stop "Neues Rathaus"	
	17:45	Forschungszentrum Jülich, Auditorium	Hotels in Jülich
			Düren Train Station

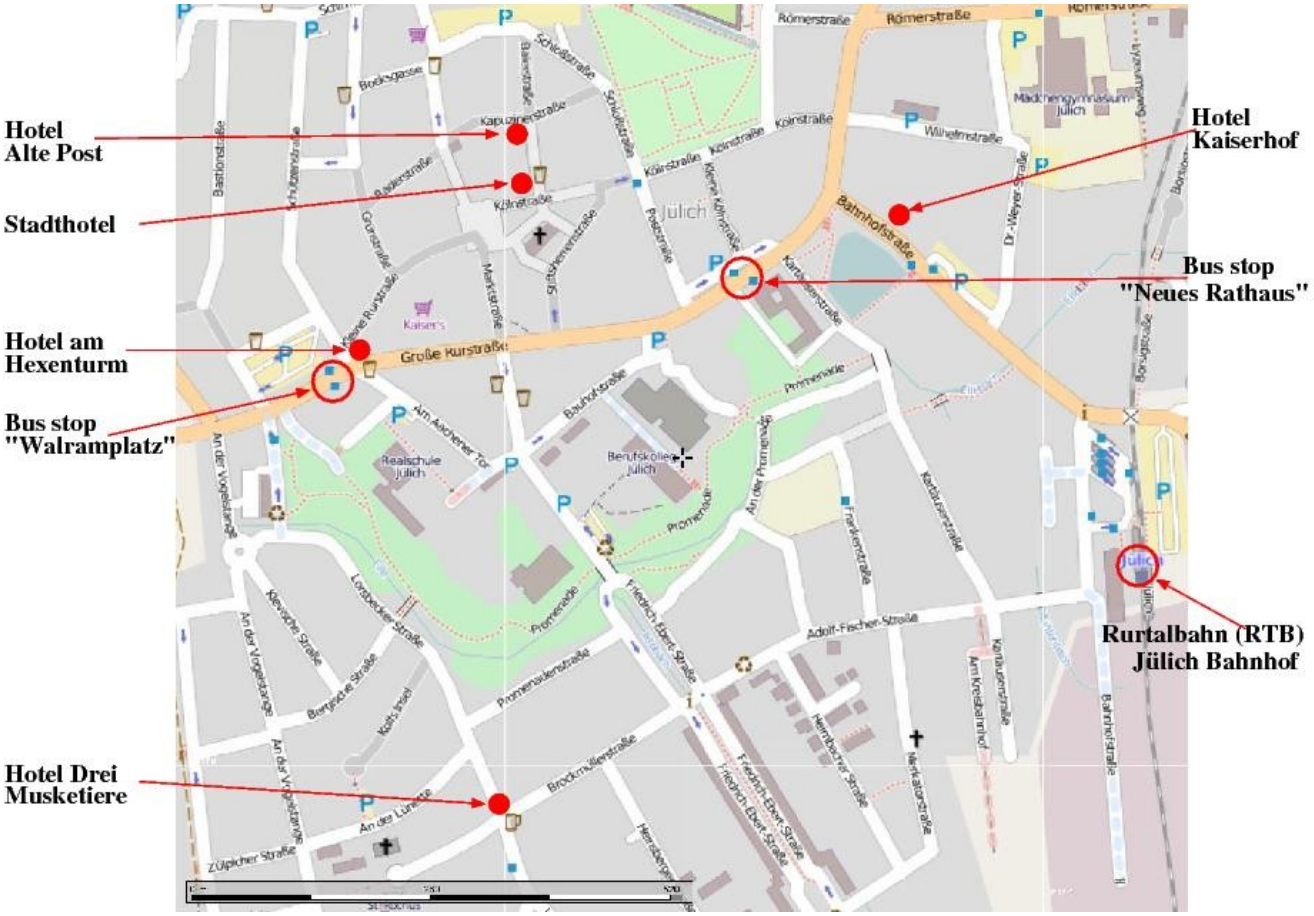

Poster Abstracts

The number in brackets in front of the title is the number of the movable wall where to place the poster for the poster session.

Elementary Particle Physics

[E 1] Continuum Limit of the Leading Order HQET Form Factor in $B_s \to K\ell\nu$ Decays

*F. Bahr, **D. Banerjee**, F. Bernardoni, A. Joseph, M. Koren, H. Simma, R. Sommer*

We discuss the computation of form factors for semi-leptonic decays of B-, B_s- mesons in lattice QCD. Considering in particular the example of the static B_s form factors we demonstrate that after non-perturbative renormalization the continuum limit can be taken with confidence. The resulting precision is of interest for extractions of V_{ub}. The size of the corrections of order $1/m_b$ is just estimated at present but it is expected that their inclusion does not pose significant difficulties.

[E 2] The Conformal Window and Technicolour Theories with Adjoint Fermions

G. Bergner

Technicolour theories are an interesting extension of the Standard Model of particle physics. In these theories the Higgs particle emerges as a bound state of a new strongly interacting sector. These strong interactions must be considerably different from quantum chromodynamics (QCD), the well known strong interactions of nuclear matter. Therefore theories with fermions in the adjoint representation play an essential role. First principle calculations of these kind of theories are only possible with intense numerical simulations. In this contribution I will review our approach and results concerning different theories with fermions in the adjoint representation. I will show how a particle spectrum much different from QCD is obtained in the numerical simulations.

[E 3] The Light Bound States of Supersymmetric SU(2) Yang-Mills Theory

*G. Bergner, **P. Giudice**, I. Montvay, G. Münster, S. Piemonte*

Supersymmetry provides a well-established theoretical framework for extensions of the standard model of particle physics and the general understanding of quantum field theories. We summarise here our investigations of N=1 supersymmetric Yang-Mills theory with SU(2) gauge symmetry using the non-perturbative first-principles method of numerical lattice simulations. The strong interactions of gluons and their superpartners, the gluinos, lead to confinement, and a spectrum of bound states including glueballs, mesons, and gluino-glueballs emerges at low energies. For unbroken supersymmetry these particles have to be arranged in supermultiplets of equal masses. In lattice simulations supersymmetry can only be recovered in the continuum limit since it is explicitly broken by the discretisation. We present the first continuum extrapolation of the mass spectrum of supersymmetric Yang-Mills theory. The results are consistent with the formation of supermultiplets and the absence of non-perturbative sources of supersymmetry breaking. Our investigations also indicate that numerical lattice simulations can be applied to non-trivial supersymmetric theories.

[E 4] Isospin Breaking Effects in QCD+QED

*Sz. Borsanyi, S. Dürr, Z. Fodor, **C.Hoelbling**, S. Katz, S. Krieg, L. Lellouch, T. Lippert, A. Portelli, K. Szabo, B. Toth*

We have computed, from first principles, the strong and electromagnetic isospin splitting in the light baryon spectrum. We have implemented the Hayakawa-Uno formulation of QED on the lattice, proven that it possesses a transfer matrix and computed the power-law finite volume effects up to $O(1/L^3)$. We have found an efficient updating algorithm for QED and a renormalization scheme for α based on the gradient flow, which allow us to reliably interpolate to the physical point. Our results imply the variation of the proton-neutron splitting due to variation of the fundamental parameters. We also predict the mass splitting for the doubly charmed baryon Ξ_{cc}.

[E 5] Search for a Bound H-Dibaryon in Two Flavour Lattice QCD

*A. Francis, J. Green, P. **Junnarkar**, C. Miao, T. Rae, H. Wittig*

We present preliminary results from a lattice QCD calculation of the H-dibaryon using two flavors of *O(*a) improved Wilson fermions. We employ six-quark interpolating operators with the appropriate quantum numbers of the H-dibaryon and also explore its couplings to two-baryon channels. To improve the overlap to the ground state two smearings are employed and a generalised eigenvalue problem is solved in the aforementioned operator basis.
With the application of Lüscher's finite volume formalism, we explore the nature of the infinite volume interaction of the two baryons. The relevant correlators are projected to three moving frames further enabling the isolation of the infinite volume bound/scattering state. Preliminary results on pion mass of 1 GeV indicate the H-dibaryon is bound in the infinite volume. Results at a lower pion mass of 451 MeV will also be presented.

[E 6] Simulations of Charm Quarks: Decoupling at Low Energies and Charmonium

***F. Knechtli**, S. Calì, T. Korzec, B. Leder, G. Moir, R. Sommer*

We study the effects of a dynamical charm quark in lattice quantum chromodynamics. To this end we simulate a model consisting of Nf=2 dynamical heavy quarks whose mass M reaches up to the charm quark mass. At energies much below M, the heavy quarks decouple. Their effects can be described by an effective theory with the heavy quarks removed. We compare the simulation results with predictions of the effective theory. Sub-percent precision is required to resolve the effects of a dynamical charm quark in low energy observables. We also study another class of observables containing valence charm quarks. Here the focus is on the control of cut-off effects which are known to be large in quantities like the hyperfine splitting. We perform direct simulations at the charm quark mass for very small values of the lattice spacing (a=0.034 fm and a=0.024 fm). We present first results on the spectrum of charmonium.

[E 7] The Electric Dipole Moment of the Neutron

*F.-K. Guo, R. Horsley, U.-G. Meissner, Y. Nakamura, **H. Perlt**, P. E. L. Rakow, G. Schierholz, A. Schiller, J. M. Zanotti*

We compute the elctric dipole moment d_n of the neutron from fully dynamical simulation of lattice QCD with 2+1 flavors of clover fermions and nonvanishing θ term. We find d_n = -3.9(2)

(9) x 10^{-16} θ e cm, which, when combined with the experimental limit on d_n, leads to the upper bound $|\theta| \leq 7.4 \times 10^{-11}$.

[E 8] Multigrid Preconditioning for the Overlap Operator in Lattice QCD

J. Brannick, A. Frommer, K. Kahl, B. Leder, M. Rottmann, ***A. Strebel***

The overlap operator is a lattice discretization of the Dirac operator of quantum chromodynamics (QCD), the fundamental physical theory of the strong interaction between the quarks.
As opposed to other discretizations, it preserves the important physical property of chiral symmetry, at the expense of requiring much more effort when solving systems posed with this operator. We present a preconditioning technique based on another lattice discretization, the Wilson-Dirac operator. The mathematical analysis precisely describes the effect of this preconditioning in the case that the Wilson-Dirac operator is normal. Although this is not exactly the case in realistic settings, we show that current smearing techniques indeed drive the Wilson-Dirac operator towards normality, thus providing motivation for why our preconditioner works well in practice. Results of numerical experiments in physically relevant settings show that our preconditioning yields accelerations of more than an order of magnitude compared to unpreconditioned solvers.

[E 9] Hadronic Corrections to the Muon Magnetic Moment

K. Szabo

The deviation of the experimental value of the anomalous magnetic moment of the muon (a_μ) compared to the value predicted by the standard model of particle physics suggests the existence of physics beyond the standard model. Here we calculate the *connected* contribution of the leading-order hadronic correction to a_μ. The current target is to reach 1-2 % accuracy. We use staggered quarks at the physical point using five lattice spacings down to 0.06 fm.

[E 10] The QCD Phase Transition with Two Quark Flavours

F. Cuteri, C. Czaban, O. Philipsen, ***C. Pinke****, A. Sciarra*

The QCD phase diagram, specifying the form of strongly interacting matter as a function of temperature and density, is important in many disciplines of physics. Finite densities are not amenable to standard Monte Carlo simulations and knowledge of the phase diagram remains scarce. We report from a long term project to determine the phase diagram of QCD with two mass degenerate quark species at zero and imaginary chemical potential, where there is no sign problem, in order to constrain the phase diagram of physical QCD at real chemical potential.

Atomic/Nuclear Physics

[AK 1] Interaction Effects on Dynamical Localization in Driven Helium

F. Joerder, K. Zimmermann, A. Rodriguez, A. Buchleitner

Dynamical localization prevents driven atomic systems from fast fragmentation by hampering the excitation process. We present numerical simulations within a collinear model of microwave-driven helium Rydberg atoms and prove that dynamical localization survives the impact of electron-electron interaction, even for doubly excited states in the presence of fast autoionization. We conclude that the effect of electron-electron repulsion on localization can be described by an appropriate rescaling of the atomic level density and of the external field with the strength of the interaction [1].

[1] F. Joerder, K. Zimmermann, A. Rodriguez, A. Buchleitner, Phys. Rev. Lett. 113, 063004 (2014).

Materials Science

[MAT 1] Electronic and Structural Properties of Dislocations in the Solar Absorber Materials CuInSe2 and CuGaSe2

***D. Barragan-Yani**, K. Albe*

In contrast to what is known for solar cells based on other semiconductor materials, current CIGS-based solar cells are able to reach power-conversion efficiencies of more than 15% while exhibiting experimental dislocation densities up to 10^{10} to 10^{11} cm^{-2}. This finding suggests that dislocations in the later are electrically not active or passivated by point defects. In order to understand the role of dislocations in CIGS-absorbers, we focus on the structures found in experiments, namely the perfect screw and 60° dislocations and the interstitial Frank loop. We do so in both CuInSe2 and CuGaSe2 by means of first-principles calculations within density functional theory. We present results on structural and electronic properties and compare formation energies of different dislocation types. It is found that all dislocations under study induce localized-shallow defect states, while two deep defect states are found for the glide 60° dislocation in CuInSe2. Due to dangling bonds presence in the dislocation types with an edge character, the perfect 60° and the Frank partial bounding the loop, we found accumulation of charge in the surroundings of those cores for both p-type and n-type conditions. Interaction with point defects, known to be common in CuInSe2 and CuGaSe2, is then enhanced. We found evidence that accumulation and depletion of copper and the presence of sodium atoms would help to passivate the charged cores. Furthermore, this non-stoichiometry induces the formation of a barrier for holes due to an offset between the valence band maximum at the cores and the corresponding value in the surrounding bulk. These results give an initial step towards understanding, why high densities of dislocations appear not to be detrimental for the efficiency of such devices.

[MAT 2] Towards Understanding Light Induced Pattern Formation: Multiscale Molecular Dynamics Study of Photoresponsive Azo-Materials

***M. Böckmann**, N. L. Doltsinis*

An increasing number of photoresponsive smart materials is made from polymers that contain azobenzene (AB) as their photochromic unit.
In this contribution, we report on our studies of the photoswitchable polymer poly-disperse-orange-3-metacrylamide (PDO3M) that we have investigated using a recently developed atomistic force field which is derived from nonadiabatic hybrid *ab initio*/classical force field (QM/MM) moleculer dynamics and includes MM-switches for both the E→Z and the Z→E photoisomerisation of AB.
PDO3M has been shown to be a successful candidate for inscribing light induced patterns (surface relief gratings, SRG) in thin film layers. Here, we investigate the microscopic mechanism of such light-induced pattern formation by repeated E↔Z photoactivation cycles of a selected region of a large periodic PDO3M surface slab while leaving the remaining region in the dark.
In comparison to a corresponding reference calculation with thermal heating, valuable conclusions of the SRG formation mechanism can be drawn.

[MAT 3] *Ab Initio* Description of Absorption, Transport and Recombination at Defective Interfaces in Solar Cells

***P. Czaja**, U. Aeberhard, M. Celino, S. Giusepponi*

We use a multi-scale approach to link the local micro-structure to the macroscopic optoelectronic properties of novel solar cell architectures, such as the a-Si:H/c-Si interface in silicon-heterojunction cells. In particular, the impact of material inhomogeneities such as structural defects and interfaces on generation, transport and recombination in a-Si:H and a-Si:H/c-Si structures is to be investigated.
To this end, atomic configurations for a-Si:H and a-Si:H/c-Si interfaces with up to 578 atoms are generated using the molecular-dynamics code CPMD. Electronic structure calculations using DFT+GW, as implemented in the electronic structure codes Quantum Espresso and BerkeleyGW, are then applied to these configurations in order to obtain the electronic wave functions and densities of states, which will be used in the *ab initio* calculation of the material properties that determine the macroscopic device characteristics (absorption coefficient, transport coefficients, recombination rates).
Since the inclusion of many-particle interactions beyond mean-field DFT is computationally extremely challenging for such a large number of atoms, we start with an independent-particle approximation, and then increase the computational complexity by taking into account quasi-particle corrections within G0W0, electron-hole interactions by means of solving the Bethe-Salpeter equation, and electron-phonon interactions.

[MAT 4] Calculation of Key Properties for Intercalation Type Electrode Materials for Li-Ion Batteries

***S. O. Dang**, R. Spatschek, L. Singheiser*

Battery research of the Li-ion chemistry continues to be of great importance due to the expansion of the market for mobile applications and the development and commercialization of electric/hybrid electric vehicles (EVs/HEVs). Moreover, the development of large scale energy storage devices has become an urgent need for further integration of renewable energy systems such as solar and wind. Because these energy generation systems cannot guarantee continuous energy supply, the integration of batteries can increase the generation flexibility and help create further economic incentives for their adoption. The driving force for the investigations into better batteries is the need for both higher power and longer lasting batteries. In the short-term and mid-term further improvements into Li-ion batteries (LIBs) can be of great importance due to the already established expertise in engineering these type of batteries.
DFT calculations were employed to model key properties of intercalation compounds for lithium ion batteries focussing on two compounds: the commercially available cathode material LixCoO2 and the potential silicon based anode material LixMg2Si.
Appropriate battery thermal management will be of vital importance to improve safety by means of mitigating thermal cascade reactions. For this purpose data on heat capacity for Lithium-transition-metal oxides can complement the array of properties needed for the analysis and modeling of temperature evolution and distribution within a battery module. Because obtaining thermodynamic properties for delithiated compounds presents a major obstacle for caloric measurements over wide temperature ranges, in this study we employ phonon calculations to obtain isobaric heat capacities within the quasi-harmonic approximation for three stoichiometries of LixCoO2.
LixMg2Si was investigated in terms of host lattice stability as a functions of lithium content to evaluate its suitability for battery applications.
For both LixCoO2 and LixMg2Si the voltage profile was derived from *ab initio* and compared to experimental data.

[MAT 5] Nucleation of Graphene on the Ge(001) p2x2 Surface

***J. Dąbrowski**, G. Lippert, G. Lupina*

Graphene microelectronics will expectedly complement the mainstream Si technology, CMOS, instead of replacing it. The reason is cost-efficiency, but the available growth methods are not easily CMOS-integrable. Large area graphene that can be grown on Cu or on Ni must be transferred onto Si(001); this is problematical due to the residual metallic contaminations [1], eg. A process in which graphene grows directly on a Si wafer would be welcome; yet SiC formation makes this hard to realize. An approach bypassing some of these problems is chemical vapor deposition (CVD) on Ge substrates [2-6]. We discuss the results of *ab initio* density functional theory (DFT) calculations for the interaction between C, H, and Ge during deposition of C2H4 on Ge(001)-p(2×2). According to our modelling, Ge dimer vacancies are found to play an important role in the process of graphene nucleation: they catalyse the polymerization process of the molecules adsorbed on the surface.

[1] G. Lupina et al., Residual Metallic Contamination of Transferred CVD Graphene, ACS Nano, 9, 4776 (2015).
[2] G. Wang et al. Direct growth of graphene film on Ge substrate. Sci. Rep. 3, 2465 (2013).
[3] J. H. Lee et al., Wafer-scale growth of single-crystal monolayer graphene on reusable H-terminated Ge, Science 344, 286 (2014).
[4] R. M. Jacobberger et al., Direct oriented growth of armchair graphene nanoribbons on Ge, Nature Comm. 6, 8006 (2015).
[5] B. Kiraly et al., Electronic and Mechanical Properties of Graphene-Ge Interfaces Grown by CVD, Nano Lett. 15, 7414 (2015).
[6] J. Dabrowski et al., Initial State of Graphene Growth on Ge(001) Surfaces, ECS Trans. 69, 345 (2015).

[MAT 6] Morphology-Transport Relationships for Porous Media

***D. Hlushkou**, H. Liasneuski, S. Khirevich, U. Tallarek*

This work describes individual steps of an approach toward quantitative correlations between morphological and mass transport properties of porous media. We show that morphology descriptors based on (i) statistical analyses of Voronoi and Delaunay cells obtained from spatial tessellation, (ii) the three-point microstructural parameter calculated from two- and three-point correlation functions, and (iii) a k-Gamma function describing a chord length distribution (i.e., a linear surface-to-surface distance distribution) allow to characterize and evaluate the effective diffusion coefficient as well as asymptotic value and transient behavior of the hydrodynamic dispersion coefficient. The presented approaches are applicable to analyze both computer-generated and physically reconstructed porous media and promise a great potential for the derivation of quantitative structure-transport relationships for heterogeneous materials, in general.

[MAT 7] Nucleation and Propagation of Shear Bands in Metallic and Network-Forming Glasses

***R. Jana**, L. Pastewka*

Molecular Dynamics simulations (MD) were used to study nucleation and propagation of shear bands during simple shear deformation of CuZr binary bulk metallic glasses (BMG), amorphous silicon (a-Si) and amorphous carbon (a-C). We find that the initial shear bands in a-Si and a-C are more localized than those found in CuZr. This localization is also found in the

spatial displacement-displacement correlation function before the onset of shear-banding. While shear bands in a-Si and a-C can be easily morphologically distinguished from their bulk by simple parameters such as the local coordination number and density, such a clear signature of shear-banding is not found in local topological parameters for CuZr, such as short-range order (SRO) determined by Voronoi tessellation. We find that thermal effects show impact on the shear localization, as shear bands vanish at elevated temperatures even below Tg.

[MAT 8] Large Scale Simulations of Nuclear Materials

***Y. Ji**, Y. Li, G. Beridze, P. M. Kowalski*

We perform atomistic simulations of radionuclide-bearing materials important for management of nuclear waste. Using large supercomputing resources provided by Forschungszentrum Jülich and RWTH Aachen we investigate kinetic processes in ceramic nuclear waste forms and irradiated nuclear graphite. We present results of simulations of radiation damage cascades in monazite-type ceramics and discuss the atoms dislocation probabilities and the threshold displacement energies. The obtained energies are substantially different from the generic values assumed by software used for simulation of irradiation experiments (e.g. SRIM code). We show the results of simulation of critical amorphization dose and compare them to the available experimental data. Because nuclear graphite represents significant amount of nuclear waste we perform large scale simulations of this material. We discuss the graphite surface chemistry, including adsorption of water and methane on the ideal and defected surfaces. We also discuss the diffusion processes of different species in graphite, including the self-diffusion of radioactive carbon (14C). Results of these simulations are confronted with the available experimental data and used for better interpretation of the experimental findings.

[MAT 9] Oxygen Vacancy Diffusion in Sodium Bismuth Titanate Studied by Density Functional Theory Calculations

***K.-C. Meyer**, M. Gröting, K. Albe*

Sodium bismuth titanate ($Na_{0.5}Bi_{0.5}TiO_3$, NBT) is a ferroelectric relaxor-like material at room temperature and has interesting electrical properties for application as a high strain actuator material. It shows a broad diffuse phase transition from a ferroelectric (rhombohedral / monoclinic) structure to a weakly polar (tetragonal) state. Recently, it has been shown that doped NBT exhibits a high ion conductivity, in contrast to other perovskites [1]. Thus, in this work we investigate by means of density functional theory calculations oxygen vacancy formation energies, association energies with different metal ions and migration barriers for different A-cation orders. We find among other things that the chemical order plays a strong role on the atomistic level, eg. for local phase transitions [2] and conductivity.

[1] M. Li, et al., Nat. Mater. 13, 31 - 36 (2014)
[2] K.-C. Meyer, et al., J. Solid State Chem. 227, 117 - 122 (2015)

[MAT 10] Quasi-Atom-Theory Inspired Potentials

*J. Jalkanen, S. Sukhomlinov, **M. Müser***

We present a systematic analysis of quasi-atom-theory (QAT) inspired potentials, which allow one to represent many-body effects in atomistic simulations without explicit many-body terms, thereby keeping the computational cost of QAT potentials close to that of two-body potentials.

Our work allows one to rationalize why different conventional QAT-type potentials, such as the embedded-atom method (EAM), do not allow one to optimize the description of defect energies independently of that of elastic properties. We also demonstrate how to systematically generalize EAM in the spirit of QAT such that many intrinsic shortcomings of EAM are eliminated. Polonium, which is the only element having the simple cubic lattice as the ground state, serves as a reference for our method.

[MAT 11] Anisotropic Magnetothermopower in Co-Based Trilayers: How Do Compare Cu, Pd, and Pt as Heterostructure Partners

V. Popescu, *P. Kratzer*

Within the framework of the spin-polarized relativistic Korringa-Kohn-Rostoker Green's function method we investigate the magnetothermopower (MTP) in a series of M/Co/M (M=Cu, Pd, and Pt) trilayer systems. As thermoelectric analogue of the conventional anisotropic magnetoresistance (AMR), the amplitude of the MTP signal is shown to depend on the asymmetry of the AMR around the Fermi energy. This asymmetry is sizable even if the magnetic layer itself displays only a small AMR, thus providing a path towards an efficient spin read-out thermoelectric device based on a single ferromagnetic layer. Our calculations establish a direct correlation between the strength of the spin-orbit coupling, modulated by the heterostructure partner M, and the MTP. The role of Co/M interface related effects such as structural relaxation and interdiffusion is also discussed.

[MAT 12] DFT-Based Reference Parameters for Solid-State NMR on Li-Ion Batteries

C. Scheurer*, Si. Köcher, M. Schuderer, J. Granwehr, K. Reuter , R. Eichel*

In operando Nuclear Magnetic Resonance (NMR) spectroscopy is a powerful tool to gain a detailed understanding of the fundamental dynamical processes inside an operating battery cell [1]. Notwithstanding, the experimental spectra are complex and their unambiguous interpretation has to rely on independent first-principles based simulations, which we establish for ^{6,7}Li solid-state NMR through density-functional theory (DFT) calculations [2]. For studies of the ionic charge carrier mobility in lithium titanium oxide ($Li_4Ti_5O_{12}$, LTO) by ^{7}Li spin-alignment echo (SAE) NMR [3], we provide first-principles reference values for chemical shielding and quadrupolar coupling. The simulations facilitate the correlation of the SAE data to Li hopping between specific crystallographic sites and provide additional insight in the Li mobility in LTO.
Electrochemically important oxygen vacancies in LTO pose a challenge to DFT calculations, since they require computationally expensive hybrid DFT calculations to reproduce the localized charge compensation by reduction of Ti^{4+} to Ti^{3+} cations. We present first results for LTO structures with oxygen deficiencies and approaches to reduce the computational effort.

[1] B. Key et al., J. Am. Chem. Soc. 131, 9239 (2009)
[2] C. Bonhomme et al., Chem. Rev. 112, 5733 (2012)
[3] M. Graf et al., submitted

[MAT 13] Strength and Failure of Steels

R. Spatschek*, C. Hüter*

The heart of many materials, including steels, is the microstructure, i.e. the spatial arrangement of different phases, grains and defects. It is central for many properties,

including strength and toughness. Microstructures are determined by thermodynamic and kinetic properties, and often the change of the microstructure during the operation and production of material is central. Therefore, a thorough understanding and numerical prediction of equilibrium and non-equilibrium microstructures and their evolution is of highest importance for progress in development of novel materials.
Hydrogen embrittlement can lead to detrimental material failure in particular of high strength steels. Already very low amounts of hydrogen in the ppm range can lead to complete failure. We link *ab initio* and atomistic to continuum descriptions to understand the thermodynamics and kinetics of nanoscopic hydride formation and their role on material failure.
Press hardening, also known as hot stamping, has become an important processing technology for the production of high strength steels mainly for automotive industry. Driven by the demand for improved crash safety and simultaneous weight reduction for fuel saving aspects, it has emerged as a major technology for the production of central parts like A- and B-pillars, bumpers or roof rails. Recent developments use interrupted cooling plus quasi isothermal holding in the bainite region, yielding partly bainitic structures with very attractive properties. This technique is called bainitic press hardening and it offers advanced strength-failure-strain combinations. However, the exact kinetics of bainite formation, in particular under large strains, is still under debate and is investigated by continuum approaches.

[MAT 14] KKRnano: Method and Code for Density-Functional Calculations for Thousands of Atoms

***R. Zeller**, P. Baumeister, S. Blügel, M. Bornemann, P. H. Dederichs, T. Fukushima, T. Hater, R. Kováčik, M. Ogura, E. Rabel, A. Thiess*

Due to the advance of supercomputing power, electronic-structure calculations for systems with more than one thousand atoms are possible today by standard density-functional codes. For larger systems their applicability, however, is severely limited because the computational effort scales with the third power of the number of atoms. Our newly developed code KKRnano overcomes this limitation by using a linear-scaling implementation of the Kohn-Korringa-Rostoker band-structure method. The basic principles of the implementation will be explained and the suitability of KKRnano for GPU processing and for more than a million parallel tasks on JUQUEEN will be demonstrated. Applications for small angle grain boundaries in SrTiO3, for high entropy alloys and for amorphous phase change materials will be discussed.

Condensed Matter

[KM 1] Optical Simulation of Tailored Disorder for Nanophotonic Thin-Film Solar Cells

A. Hoffmann, ***M. Ermes****,* ***K. Bittkau***

Thin-film solar cells demand for advanced light-trapping concepts, in order to overcome limitations due to weak absorptance near the band gap. One common concept is incorporating random textures that scatter incoming light diffusely prolonging the effective light path in the absorber layer in a broad spectral range. Furthermore, periodic grating structures incorporated at different interfaces of the device are investigated by several groups. By those periodic structures, the excitation of waveguide modes improves the external quantum efficiency (EQE) in narrow spectral ranges.
We have recently demonstrated experimentally that by introducing tailored disorder into the two-dimensional grating structure, the spectrally sharp resonances of the waveguide modes are broaden which leads to an improved EQE in a broad spectral range. The solar cells on those disordered gratings show a higher EQE compared to reference cells on state-of-the-art random textures. As the parameter space for disordered gratings is large, the optimization of those textures is hard to achieve only by experiment.
Therefore, we investigated in this contribution the impact of tailored disordered grating structures on the EQE by applying the Finite-Difference Time-Domain method. We used a hydrogenated amorphous silicon thin-film solar cell in superstrate configuration as a test structure. The thickness of the absorber layer is 250 nm. The disorder is tailored by different ways, e.g. by a variation of the particle position within the unit cell, the radius of the particles or their heights. The simulations are done in the relevant spectral range for light trapping with a spectral resolution of 2 nm in order to resolve the resonances accurately.
The experimental results are nicely reproduced by simulations. The detailed simulation series shows a trade-off between the resonant enhancement effect of waveguides and a spectral broadening due to disorder. This provides routes to further improve light trapping in thin-film solar cells.

[KM 2] Thermal Phase Transitions in the Vicinity of the Quantum Critical Point of Spinless Fermions on the Honeycomb Lattice

S. Hesselmann*, S. Wessel*

We consider spinless fermions on a honeycomb lattice (spinless t − V model), which provide a minimal realization of lattice Dirac fermions. Nearest neighbor interactions drive a quantum phase transition from a semi-metallic phase to a charge ordered phase, which spontaneously breaks the chiral Z_2 symmetry of the Dirac fermions. The critical theory is given by the Gross-Neveu-Yukawa theory, which describes the process of mass generation due to the broken chiral symmetry. At finite temperature (and $V > V_c$) the quantum critical point connects to a line of second order thermal phase transitions that restore the broken chiral symmetry. We employ a recent sign-problem-free continuous time quantum Monte Carlo method [1,2] to investigate the finite temperature phase diagram of the model. Furthermore we give estimates for the critical exponents of the Gross-Neveu chiral Ising universality class by studying the extension of the quantum critical regime to finite temperatures.

[1] E. F. Huffman et al., Phys. Rev. B 89, 111101(R) (2014).
[2] L. Wang et al., New J. Phys. 16, 103008 (2014).

[KM 3] Comparability of Microcanonical Data Sampled by Molecular Dynamics and Monte Carlo Simulations

P. Schierz, J. Zierenberg, ***W. Janke***

In this work we performed microcanonical simulations with statistical Monte Carlo (MC) sampling and dynamical Molecular Dynamics (MD) integrations. Our aim was to get both methods into agreement which needed a careful consideration of the conservation laws one encounters in MD simulations. We applied a time series reweighting technique to transform the MD sampling to the full NVE ensemeble without conservation laws. For a higher number of degrees of freedom the differences between the simulation techniques diminished as expected. We adapted the known weighted histogram analysis method (WHAM) to be applicable to microcanonical MD simulation data. By this means we arrived at an estimate for the density of states from MD simulations. This procedure requires an accurate knowledge of the sampled statistical ensembles.

P. Schierz, J. Zierenberg, and W. Janke, J. Chem. Phys. 143, 134114 (2015).

[KM 4] Approximate Validity of the Jarzynski Relation for Non-Gibbsian Initial States in Isolated Systems

F. Jin*, R. Steinigeweg, H. De Raedt, K. Michielsen, M. Campisi, J. Gemmer*

Since the first suggestion of the Jarzynski equality many derivations of this equality have been presented in both, the classical and the quantum context. While the approaches and settings greatly differ from one to another, they all appear to rely on the initial state being a thermal Gibbs state. Here, we present an investigation of work distributions in driven isolated quantum systems, starting off from pure states that are close to energy eigenstates of the initial Hamiltonian. We find that, for the nonintegrable system in quest, the Jarzynski equality is fulfilled to good accuracy.

[KM 5] Tuning the Optical Spectrum of Carbon Nanotubes by the Environment

M. Rohlfing

The optical spectra of nanostructured systems can be manipulated (e.g., red-shifted) when the environment is changed, e.g. by physisorbed material, even without chemical modification.
The spectrum of a carbon nanotube (CNT) can be red-shifted by several 10 meV by environmental polarizability, e.g. from another CNT at touching distance (see the figure for peak shifts in the visible spectrum of several (N,0) CNTs [1]), or by the admixture of charge-transfer configurations [1,2]. Similar effects are observed in layered materials, like graphene/graphite of boron nitride.Spectra can also be modified by atomic adsorbates, like oxygen or hydrogen atoms on the surface of a CNT [3].We discuss all these effects in terms of the Bethe-Salpeter equation (BSE) for electron-hole pair states on the basis of a preceding GW calculation.

[1] M. Rohlfing, Phys. Rev. Lett. 108, 087402 (2012).
[2] H. Yin, Y. Ma, J. Mu, C. Liu, and M. Rohlfing, Phys. Rev. Lett. 112, 228301 (2014).
[3] J. Mu, Y. Ma, H. Yin, C. Liu, and M. Rohlfing, Phys. Rev. Lett. 111, 137401 (2013).

[KM 6] Simulation of Quantum Mechanical Many-Fermion Systems

***S. Trebst**, P. Broecker, M. Gerlach*

We discuss recent results from project HKU22 "Simulation of quantum mechanical many-fermion systems", which attacks the many-fermion problem from a variety of angles. Here, we will report on (i) the investigation of competing orders at the onset of antiferromagnetism in metals [1] and (ii) the connection of quantum mechanical entanglement and the fermion-sign problem in auxiliary-field Monte Carlo simulations [2].

[1] Yoni Schattner, Max H. Gerlach, Simon Trebst, and Erez Berg, Competing Orders in a Nearly Antiferromagnetic Metal, preprint arXiv:1512.07257
[2] Peter Broecker and Simon Trebst, Entanglement and the fermion sign problem in auxiliary field quantum Monte Carlo simulations, preprint arXiv:1511.02878

Computational Soft Matter Science

[POLY 1] Static and Dynamic Properties of Polymer Melts: Equilibrium and Non-Equilibrium Molecular Dynamics Studies

H.-P. Hsu *,K. Kremer*

We present a detailed study of the static and dynamic behavior of semiflexible polymer chains in a melt starting from the previously obtained fully equilibrated high molecular weight polymer melts by a hierarchical strategy [1,2]. For semiflexible chains in a melt, we see that results of the mean square internal distance, the probability distributions of the end-to-end distance, and the chain structure factor are all described by the theoretical predictions for ideal chains to some extent. We examine the motion of monomers in polymer melts by molecular dynamic (MD) simulations using the ESPResSo++ package [3]. The scaling predictions of the mean square displacement of inner monomers, center of mass, and the relative behavior between them based on the Rouse model, and the reptation theory are verified, and the related characteristic relaxation time scales are determined. We also check the topological structures of polymer chains through the primitive path analysis (PPA) [4], and give the evidence that the entanglement length determined through PPA in the standard expression of the plateau modules is consistent with the value obtained from stresses using the Green-Kubo relation [5]. Finally, the non-linear viscoelastic properties of deformed polymer melts after a step uniaxial elongation and the conformational changes of chains during the relaxation process are investigated through a non-equilibrium MD study.

[1] G. Zhang, L. A. Moreira, T. Stuehn, K. Ch. Daoulas, and K. Kremer, ACS Macro Lett. 3, 198 (2014).
[2] G. Zhang, K. Ch. Daoulas, and K. kremer, Macromol. Chem. Phys. 214, 214 (2013) Macromolecules, 43, 1592 (2010).
[3] *ESPresSo++*: J. D. Halverson, T. Brandes, O. Lenz, A. Arnold, S. Bevc, V. Starchenko, K. Kremer, T. Stuehn, and D. Reith, Comput. Phys. Commun. 184, 1129 (2013).
[4] R. Everaers, S. K. Sukumaran, G. S. Grest, C. Svaneborg, A. Sivasubramanian, and K. Kremer, Science 303, 823 (2004).
[5] H.-P. Hsu, and K. Kremer, preprint (2016).

[POLY 2] Desorption Energy of Soft Particles from a Fluid Interface

H. Mehrabian*, J. H. Snoeijer, J. Harting*

Soft particles are considered to be better stabilizers for emulsions due to their stronger attachment to a fluid interface. Using constrained molecular dynamics simulations and the thermodynamic integration method, desorption energy of soft gel-like particles from a fluid interface is calculated. It is shown that the model can correctly reproduce the detachment work of a rigid particle. Role of the particle softness and surface tension on the desorption energy is studied. Contrary to the common belief about the desorption energy of soft particles, it is shown that the higher softness of the particle does not affect the maximum force required to detach the particle from the interface, and it does not change the detachment work significantly. For swollen gel particles, it is shown that both the detachment work and maximum detachment force increases considerably compared to rigid particles.

[POLY 3] Process-Directed Self-Assembly of Copolymer Materials

W. Li, J.-C. Orozco Rey, D.-W. Sun, J. Tang, U. Welling, ***M. Müller***

Using computer simulations of a soft, coarse-grained particle model and numerical self-consistent field calculations, we study the kinetics of self-assembly and defect annihilation in block copolymers. The minimum free-energy path of defect annihilation and non-bulk-like structures are discussed, and the role of non-equilibrium single-chain conformations, conserved densities and dependence of the complex free-energy landscape on the thermodynamic state are highlighted.

[POLY 4] Interfacial Growth in a Binary Polymer Mixture: A Modified External Potential Dynamics and Brownian Dynamics

S. Qi*, F. Schmid*

The dynamic mean-field density functional theory is widely used studying phase transitions in polymer systems. Especially, the external potential dynamics (EPD) is demonstrated to be powerful and computationally more efficient. For example, based on Rouse dynamics, the dynamic self-consistent field theory and EPD can give almost identical predictions in describing the spinodal decomposition in a binary incompressible polymer mixture, while the EPD is computationally more efficient. In the present study, we focus on the interfacial broadening and sharpening in a compressible binary polymer blend. We found that in this case, the density dynamics would capture the main feature of the interfacial growth, while the EPD shows spurious dynamics, and this is verified by the BD simulations. Approximations in obtaining the the EPD equations are responsible for the discrepancy between density dynamics and EPD. We proposed a modified EPD, which can avoid the approximations in the original version of EPD, and thus leads to the correct predictions. However, this modified version of EPD is a few times slower than the density dynamics with nonlocal coupling coefficient, which is approximately expressed as Debye function. Thus density dynamics with nonlocal coupling maybe sometimes more favorable.

[POLY 5] From Amorphous Aggregates to Polymer Bundles: The Role of Stiffness on Structural Phases in Polymer Aggregation

J. Zierenberg*, W. Janke*

We study the aggregation transition of a full range of semiflexible theta-polymers using parallel multicanonical simulations [1]. This model includes self-avoidance, short-range attraction, and bending stiffness. For a single polymer, the limiting cases of weak and strong bending stiffness thus yield the self-interacting self-avoiding walk (flexible) and the rather stiff worm-like chain, respectively. This spans a range of polymer models from (flexible) synthetic polymers to (stiff) biopolymers. For more than one polymer, the mutual attractive interaction causes the formation of an aggregate, a transition that is competing with the single-polymer deformation (e.g. the collapse transition). We show that stiffness determines the motif of the aggregate, leading from amorphous aggregates to polymer bundles [2]. The transition is a first-order like transition and the accompanying free-energy barrier is shown to increase with stiffness and thus with the structural order of the aggregate. For stiffer polymers, we observed twisted bundles which recapture results from worm-like chain bundle models and from analytic treatment of twisted fibers.

[1] J. Zierenberg, M. Marenz, and W. Janke, Comput. Phys. Comm. 184, 1155 (2013).
[2] J. Zierenberg and W. Janke, Europhys. Lett. 109, 28002 (2015).

[POLY 6] Lattice Boltzmann Simulations of Electrokinetic Phenomena

S. Frijters, ***N. Rivas****, J. Harting*

Electrokinetic phenomena play a crucial role in many new technological developments, from lab-on-a-chip devices to oil exploration techniques. In the last years, computer simulations have started to provide important information where theoretical understanding has until now been poor. We focus on colloidal suspensions in electrolyte solutions, with the final goal of assessing the possibility of controlling their arrangement through external electrical fields. For this, we have extended the parallel *lb3d* Lattice-Boltzmann simulation code to integrate electrical charges and fully resolved colloids, together with their mutual interactions and with the solvents. Charge distributions are solved using the link-flux method, as proposed by Capuani et al. (2004), which allows us to resolve complex boundaries while maintaining charge conservation. The resulting electrical field is computed using the particle-particle/particle-mesh (P3M) Poisson equation solver. In this poster we describe the algorithm in more detail and show first benchmark results of the full code implementation.

Computational Plasma Physics

[PLA 1] Electron-Injection Techniques in Plasma-Wakefield Accelerators for Driving Free-Electron Lasers

*J. Osterhoff, **A. Aschikhin**, C. Behrens, L. Di Lucchio, J. Grebenyuk, Z. Hu, A. Martinez de la Ossa, J. L. Martins, T. Mehrling, L. O. Silva, J. Vieira, M. Vranic, V. Wacker, M. Weikum*

We will present results concentrating on numerical simulations of controlled injection of particle beams into plasma accelerators for producing high-brightness beams optimized for FEL applications. Since the physics involved in the process cannot be treated analytically in most of the cases of interest, particle-in-cell (PIC) simulations are required. PIC simulations allow to calculate the response of the plasma electrons to the passage of charged beams and/or high-intensity lasers by numerically solving the Maxwell equations in a box that follows the driver. The electromagnetic fields of the system are discretised on a three-dimensional spatial grid inside the box (the cells), while the individual particles are represented by the introduction of macro-particles. The computational load is distributed over a number of processors, which simultaneously solve the equations in different spatial regions of the system. This parallelisation and sharing of the work among few hundreds to ten thousands of processing units in supercomputing machines allows for a full numerical modelling of the relevant phenomena in plasma-based acceleration. We performed large-scale 3D simulations using both laser pulses and a particle beams to drive the wakefield. The parameters corresponding to available laboratory conditions for plasma based accelerators are computationally demanding and typically involve 10^5 - 10^6 CPU core hours on the high-performance computer JUQUEEN.

[PLA 2] Efficient Modeling of Matching Sections for Laser-Plasma Acceleration

***I. Dornmair**, K. Floettmann, M.Kirchen, A. R. Maier*

Laser plasma accelerators provide large accelerating gradients and thus bear the promise to significantly reduce the size and cost of particle accelerators, with possible application as drivers for brilliant light sources such as Free-Electron Lasers.
However, the accelerating fields inside the wakefield are accompanied by strong focusing fields, that cause extremely small beam size and consequently large divergence of accelerated electron bunches.
Owed to this divergence it is very challenging to capture the beam after the plasma, and, for external injection, the focusing optics before the plasma need to be very strong. Furthermore, in combination with a large energy spread, the divergence will lead to rapid beam quality degradation in a drift.
Tailored matching sections at the beginning and end of a plasma target allow to slowly increase or decrease this focusing force and thus to decrease the divergence, thereby relaxing the constraints on the beam optics. We present ideal density and laser beam evolution profiles to create these sections and show exemplary particle in cell simulations with WARP[1] of a stage for external injection.
As the target considered for this case is comparably long, significant speedup of the PIC simulation can be achieved by using boosted frame simulations. In order to get interpretable output, a Lorentz transformation to the lab frame needs to be done. Since space and time are then coupled, routines that continously transform and dump data during the simulation are implemented.

[1] A. Friedman, R. H. Cohen, D. P. Grote, S. M. Lund, W. M. Sharp, J.-L. Vay, I. Haber and R. A. Kishek, IEEE Trans. Plasma Sci. 42, 1321 (2014).

[PLA 3] Simulation of Optical Response from Plasmonic Nanostructures

***Y. Grynko**, J. Foerstner*

The problem of numerical simulation of the linear and nonlinear optical response from plasmonic nanostructures is multi-scale that makes it hard for existing numerical methods. These are subwavelength metallic objects with sizes ranging from tens to hundreds of nanometers and the mechanisms responsible for, e.g., the second harmonic generation (SHG) apparently act on scales of the order of 1 nm. We apply the Discontinuous Galerkin Time Domain method and the hydrodynamic Maxwell-Vlasov model to do such simulations for split-ring resonator and gap nano-antenna arrays. Our results are in qualitative agreement with corresponding experimental measurements of the SHG spectra.

[PLA 4] Inverse Faraday Effect Driven by Radiation Friction in Ul-Traintense Laser-Plasma Interactions

***T. Liseykina**, S. Popruzhenko, A. Macchi, D. Bauer*

In the interaction of extremely intense laser pulses with thick targets, as foreseen with next generation lasers such as ELI, radiation friction effects are expected to convert a major fraction of the laser energy into incoherent radiation. For a circularly polarized laser pulse, the radiative dissipation allows to absorb electromagnetic angular momentum, which in turn leads to the generation of an ultrastrong (Gigagauss) axial magnetic field. Such Inverse Faraday Effect driven by radiation friction in demonstrated and analyzed in three-dimensional simulations. Simple models for the efficiency of radiative losses, the transfer of angular momentum to ions and the saturation value of the magnetic field provide the estimates of these quantities which are in fair agreement with the simulation results. With the advent of multi-petawatt laser systems, the investigated effect may provide a macroscopic signature of radiation friction.

[PLA 5] Ultrafast Electron Kinetics in Short Pulse Laser-Driven Dense Targets

P. Sperling, R. Redmer

We have studied the light–matter interaction of ultra-short, intense optical and soft X-ray laser fields via particle-in-cell simulations. We consider liquid hydrogen droplets [1,2] and thin carbon foils [3] as targets which are subject of corresponding pump-probe experiments at free electron lasers such as FLASH (DESY Hamburg) and LCLS (SLAC Stanford). Besides tunnel and field ionization we have studied the influence of additional impact ionization processes on the density and temperature of the generated plasma (carbon). We have calculated the corresponding Thomson scattering spectra for various time delays up to few ps duration between the pump and probe pulse from which the plasma parameters can be extracted. In this way, the equilibration time of dense laser-generated plasmas with different electron and ion temperatures can be determined (hydrogen). These problems are the key for a better understanding of the ultra-short time kinetics in the laser-matter interaction and the subsequent relaxation phenomena.

[1] U. Zastrau, P. Sperling, et al., Phys. Rev. Lett. 112, 105002 (2014).
[2] U- Zastrau, P. Sperling, et al., Phys. Rev. E 90, 013104 (2014).
[3] P. Sperling, U. Zastrau, et al., J. Phys. B 48, 125701 (2015).

[PLA 6] Collisionless Shock Formation and Ion Acceleration in Astrophysics and in the Laboratory

A. Stockem Novo*, E. P. Alves, K. Schoeffler, L. O. Silva, R. Schlickeiser*

A shock is characterised by a jump in several physical quantities, such as the particle density, the fluid velocity or the temperature. In contrast to hydrodynamic shocks, collisionless shocks form due to the interaction of particles with electromagnetic fields. Micro turbulence is seeded due to plasma instabilities, which is then transformed to a large scale structure. In different sub-projects, we have studied the shock formation process and the mediating instabilities in astrophysical environments. Furthermore, the findings are applied to the field of laser-plasma physics in order to benefit from an interdisciplinary approach.

Computational Chemistry

[CH 1] On the Role of Interfacial Hydrogen Bonds in On-Water Catalysis

***K. Karhan**, R. Z. Khalliulin, T. D. Kühne*

It has been demonstrated that many classes of organic reactions exhibit increased reaction rates when performed in heterogeneous water emulsions [1]. This so-called “on-water” catalytic effect offers a highly promising perspective to improve reactions in organic chemistry. This is partly due to the widespread use of the catalyzed cycloaddition reaction in organic synthesis and partly due to the availability and environmental friendliness of the catalyst. Despite enormous practical importance of the observed “on-water” catalytic effect and numerous mechanistic studies [2,3] its microscopic origins remain unclear. In this work [4], we applied a second generation Car-Parrinello molecular dynamics algorithm [5] adapted for use with self-consistent density functional tight-binding [6] to perform a fully quantum mechanical calculation of the free energy barriers for Diels-Alder reaction between dimethyl-azodicarboxylate and quadricyclane. Although experimentally measured reaction rate is ∼24 times higher under the heterogeneous conditions predict the opposite trend: the calculated free energy activation barrier at the water-vacuum or water-organic interface is ∼10 kJ/mol higher than that in bulk water. Our results imply that the stabilization of the transition state by dangling hydrogen bonds exposed at aqueous interfaces plays a significantly lesser role in “on-water” catalysis than has been suggested before.

[1] S. Narayan et. al., Angew. Chem. Int. Ed. 44, 3275 (2005).
[2] L. L. Thomas et. al., J. Am. Chem. Soc. 132, 3097 (2010).
[3] Y. Jung et. al., Jour. Phys. Cond. Mat. 22, 284117 (2010).
[4] K. Karhan et. al., Jour. Chem. Phys 141, 22D528 (2014).
[5] T. D. K˙uhne et. al., Phys. Rev. Lett. 98, 066401 (2007).
[6] M. Elstner et. al., Phys. Rev. B 58, 7260 (1998).

[CH 2] Nuclear Quantum Effects in Water with Path Integral Simulations

***H. Wiebeler**, T. Spura, T. D. Kühne*

In a previous publication [1], Kühne and coworkers developed a flexible, pairwise water-model via force matching to accurate electronic structure calculations to investigate the influence of nuclear quantum effects by means of path integral molecular dynamics (PIMD) [2,3] simulations. However, there are subtle collective many-body effects, such as those arising from hydrogen bonding [4], which render the assumption of pairwise additive interactions as not accurate enough. In this work, we extend the aforementioned water model by the E3B(explicit three body)-method of Skinner and coworkers [5] and combine this with PIMD to study the water/vapor interface.

[1] T. Spura, C. John, S. Habershon and T. D. K˙uhne, Mol. Phys. 113, 808 (2015).
[2] D. Chandler and P. G. Wolynes, J. Chem. Phys. 74, 4078 (1981).
[3] M. Parrinello and A. Rahman, J. Chem. Phys. 80, 860 (1984).
[4] R. Kumar and J. L. Skinner, J. Phys. Chem. B 112, 8311 (2008).
[5] C. J. Tainter, P.A. Pieniazek, Y. S. Lin and J. L. Skinner, J. Chem. Phys. 138, 184501 (2011).

[CH 3] Theoretical Methods for Studying Long-Range Charge and Spin Separation in Excited States in Condensed Phase

***V. Ziaei**, T. Bredow*

Optical absorption spectrum of liquid water is presented in the energy range of 5–20 eV using many-body perturbation theory. Representative structures of liquid water are obtained from periodic *ab initio* Born-Oppenheimer Molecular-Dynamics simulations. Main features of recent inelastic X-ray measurements are well reproduced, such as a bound excitonic peak at 7.9 eV with a shoulder at 9.6 eV, and the absorption maximum at 13.85 eV, followed by a broad shoulder at 18.6 eV. The low energy part of the spectrum is dominated by excitonic effects which also impact the structures of the spectrum at higher energies along with single particle effects. The exciton distribution of the low-energy states, in particular of S1, is highly anisotropic and localized mostly on one water molecule. The S1 state is essentially a HOCO-LUCO (highest occupied crystal orbital - lowest unoccupied crystal orbital) transition and of intra-molecular type, showing a localized valence character with small Rydberg contributions. Once the excitation energy is increased, a significant change in the character of the electronically excited states takes place which is apparent through emergence of multiple quasi particle peaks at 7.9 eV in the quasi-particle (QP) transition profile and in the occurring delocalized exiton distribution, involving more water molecules participating actively in the excited state. For even higher excitations, near vertical ionization energy (11 eV), quasi free electrons are emerged.
Furthermore, relaxation processes, such as proton coupled electron transfer (PCET) and hot hydrogen atom (HHA) through tracking of non-adiabatic dynamics in excited states are analyzed. The net effect of relaxation processes following photo-excitation at energies below the electronic band gap is formation of an OH radical and a solvated electron through processes involving explicitly the nuclear motion of the solvent. The through low-energy processes (PCET & HHA) ejected excess charge seems to be not fully localized within a cavity of surrounding solvent molecules, in contrary to the previous one electron pseudo potential calculations. Hence, performing accurate quantum mechanical calculations for larger simulation cells is mandatory to verify the relaxation processes, the degree of localization of solvated electron and its (non-)geminate recombination dynamics.

[CH 4] Identification of Correlation Between OH* Chemiluminescence and Heat Release Rate with Direct Numerical Simulation

*F.Zhang, **T. Zirwes**, P. Habisreuther, H. Bockhorn*

Traditionally, high-speed imaging of hydroxyl (OH*) or methylidyne radical (CH*) chemiluminescence with intensified cameras is used to characterize the unsteady heat release in turbulent flames. The correlation between heat release and chemiluminescence was determined empirically. Proportionality is commonly assumed which is not based on an understanding of the underlying processes but rather sanctified by the results. Therefore, objective of this work is to quantify the connection between heat release and generation of chemiluminescence in a more precise way.
To accomplish this, direct numerical simulations (DNS) imposing complex reaction kinetics with the full reaction paths of the chemically excited OH* radicals have been applied to simulate a synthetic flame front and a turbulent jet flame. A strong correlation between the local generation of the chemiluminescent specie OH* and heat release has been confirmed, especially for lean-premixed flames. This correlation is, however, not exactly linear, but the integral or line-of-sight summed values showed a quasi-linear connection, validating the generally used proportionality relation for the prediction of heat release rate from the overall intensity of chemiluminescence emissions.
The open-source code OpenFOAM has been used to perform the DNS simulations, where

the detailed calculation of chemical reaction and transport process has been implemented in addition to its general capabilities for CFD modeling of non-reactive flows. The code is capable of solving the compressible reactive flow equations exactly, employing the finite volume method on unstructured grids. The detailed description of the chemistry, i.e. the reaction rates, and transport, i.e. the diffusion coefficients, has been accomplished by coupling with the open-source chemical kinetics library Cantera. The mixture-averaged model is used for the diffusive mass flux, the viscous stress flux of a Newtonian fluid and the diffusive heat flux. A general operator splitting technique has been used for the evaluation of chemical source terms, calculating the system of chemical reactions decoupled from the solution of the flow equations. In this case, a zero-dimensional batch reactor has been created for each discrete cell volume and the resulting kinetics equations are numerically integrated over the time step of the flow, thereby resolving the smallest time scales of the reaction system. A very good scaling behaviour of the solver has been observed on the IBM Blue Gene/Q computing architecture from JSC and the Cray XC40 machine at HLRS Stuttgart.

Computational Biology and Biophysics

[BIO 1] Carnosine and Homocarnosine Binding to their Target Carnosinase Enzyme CN1: A Comparative Computational Study

***M. Pavlin**, G. Rossetti, M. De Vivo, P. Carloni*

Alzheimer's disease (AD) is one of the incurable and progressive neurodegenerative diseases (ND). An important characteristic in the pathogenesis of AD, as well as other ND, is the dyshomeostasis of metal ions in the brain. Mainly, AD is characterized by an unbalance of Zn(II) and Ca(II) ions in glutamatergic neurons[1]. Evidences from the experiments suggest that Zn(II) enriched diet could slow the developing of the AD in young mice (1 month) however the same diet shows an opposite effect on older mice (11 month)[2]. A possible Zn(II) ligand which could be used in regulation of Zn(II) homeostasis is endogenous dipeptide L-carnosine (β-alanyl-L-histidine, Lcar). It was already shown that it can prevent and reduce several pathologies such as ALS, Alzheimers's and Parkinson's disease[3]. Unfortunately its therapeutic applications are drastically limited due to its hydrolysis by human serum and tissue carnosinase enzymes (hCN1 and hCN2)[4]. Identifying Lcar mimics that escape degradation may greatly boost its therapeutic applications. Here we investigated Lcar's and one of its derivatives, homocarnosine's (γ-amino-butyryl-L-histidine, Hcar), conformational ensembles in water by multiple microsecond molecular dynamics simulations. Quality of our simulations was established by comparison with all available NMR data. Based on this information, and using bioinformatics, as well as docking and *ab initio* simulations, we predict Lcar's and Hcar's poses in the Lcar-specific hCN1, for which the first is a substrate and the latter a competitive inhibitor[5]. We suggest that degradation of Lcar occurs through a nucleophilic attack of a Zn(II)-coordinated water molecule. This proposal differs from previous mechanistic studies, which could not rely on recently determined hCN1 structure. This knowledge can be used for further structure-aided L-carnosine mimic design.

[1] a) Corona, C. et al., Cell Death and Dis. 2011, 2, e176; b) Sensi, S., et al., J. Neurosci. 2011, 31, 16076-16085.
[2] Corona, C. et al., Cell Death and Dis. 2010, 1, e91.
[3] Boldyrev, A.A., Aldini, G., Derave, W., Physiol. Rev. 2013, 93, 1803-1845.
[4] Teufel, M. et al., J. Biol. Chem. 2003, 278, 6521-6531.
[5] Peters, V. et al., Amino Acids 2010, 38, 1607-1615.

[BIO 2] Spiking Neural Network Simulation Including Gap Junctions

***J. Hahne**, M. Helias, S. Kunkel, J. Igarashi, M. Bolten, A. Frommer, M. Diesmann*

Contemporary simulation technology for neuronal networks enables the simulation of brain-scale networks using neuron models with a single or a few compartments. However, distributed simulations with correct cell densities are still lacking the electrical coupling between cells via so called gap junctions. This is due to the absence of efficient algorithms to simulate gap junctions on large parallel computers. The reason is that current simulation codes for spiking neurons rely on delayed communication, whereas gap junctions require an instantaneous interaction between the coupled neurons. Here, we present our recently published novel approach based on a waveform relaxation technique. The framework is on the one hand compatible with the communication strategy of current spiking simulators and on the other hand provides a high accuracy for the simulation of gap junctions.

[BIO 3] Simulations for the Reconstruction of Nerve Fibers by 3D Polarized Light Imaging

***M. Menzel**, M. Axer, H. De Raedt, K. Michielsen*

The neuroimaging technique 3D Polarized Light Imaging (3D-PLI) allows to reconstruct the architecture of nerve fibers in human post-mortem brains with micrometer resolution [1-4]: Unstained histological brain sections are placed in a polarimeter that measures the birefringence (optical anisotropy) of the nerve fibers. Due to the birefringence, the light wave experiences a phase shift (retardation) when passing through the brain section [5]. As the retardation depends on the structure and geometry of the fibers, the resulting intensity profile is a direct measure of the spatial orientation of the nerve fibers.
In order to better understand the physical processes behind 3D-PLI and to improve the reliability and accuracy of the reconstructed fiber orientations, the propagation of the polarized light wave through the brain tissue is simulated by means of a massively parallel 3D Maxwell solver.
The Maxwell solver is based on an unconditionally stable Finite-Difference Time-Domain (FDTD) algorithm [6] which computes the electromagnetic field components by discretizing space and time and approximating Maxwell's equations by finite differences. The algorithm uses the formal solution of Maxwell's equations in matrix form and the Lie-Trotter-Suzuki product formula approach [7]. The simulations are performed on JUQUEEN [8].
We demonstrate that the Maxwell solver is a valuable tool to model the interaction of the polarized light wave with the brain tissue. It does not only reproduce the most dominant effects observed in a 3D-PLI measurement, but also helps to enhance the accuracy and reliability of the reconstructed fiber orientations and thus our understanding of the structural organization of the human brain.

[1] M. Axer, K. Amunts, D. Grässel, C. Palm, J. Dammers, H. Axer, U. Pietrzyk, and K. Zilles. A novel approach to the human connectome: Ultra-high resolution mapping of fiber tracts in the brain. NeuroImage, 54(2):1091-1101, 2011. doi:10.1016/j.neuroimage.2010.08.075
[2] M. Axer, D. Grässel, M. Kleiner, J. Dammers, T. Dickscheid, J. Reckfort, T. Hütz, B. Eiben, U. Pietrzyk, K. Zilles, and K. Amunts. High-resolution fiber tract reconstruction in the human brain by means of three-dimensional polarized light imaging. Frontiers in Neuroinformatics, 5(34):1-13, 2011. doi:10.3389/fninf.2011.00034
[3] M. Dohmen, M. Menzel, H. Wiese, J. Reckfort, F. Hanke, U. Pietrzyk, K. Zilles, K. Amunts, and M. Axer. Understanding fiber mixture by simulation in 3D Polarized Light Imaging. NeuroImage, 111:464-475,2015. doi:10.1016/j.neuroimage.2015.02.020
[4] M. Menzel, K. Michielsen, H. De Raedt, J. Reckfort, K. Amunts, and M. Axer. A Jones matrix formalism for simulating three-dimensional polarized light imaging of brain tissue. Journal of the Royal Society Interface, 12:20150734, 2015. doi:10.1098/rsif.2015.0734
[5] M.Born and E. Wolf. Principles of Optics – Electromagnetic Theory of Propagation, Interference and Diffraction of Light. 7th Edn., Cambridge University Press, 2011. ISBN-13:978-0-521-64222-4
[6] A. Taflove and S. C. Hagness. Computational Electrodynamics: The Finite-Difference Time-Domain Method. Artech House, MA USA, 3rd Edn., 2005
[7] H. De Raedt. Advances in unconditionally stable techniques. In A. Taflove and S. C. Hagness, Eds., Computational Electrodynamics: The Finite-Difference Time-Domain Method, Chp. 18. Artech House, MA USA, 3rd Edn., 2005.
[8] M. Stephan, J. Docter, and JUQUEEN. IBM Blue Gene/Q Supercomputer System at the Jülich Supercomputing Centre. Journal of large-scale research facilities, 1, A1, 2015. URL: http://dx.doi.org/10.17815/jlsrf-1-18

[BIO 4] Consequences of Clinically Relevant Glutamine Synthetase Mutations at the Atomic Level

***B. Frieg**, B. Görg, N. Homeyer, V. Keitel, D. Häussinger, H. Gohlke*

Glutamine synthetase (GS) catalyzes the ATP-dependent ligation of ammonia and glutamate to glutamine and, thus, is essential for nitrogen metabolism [1,2]. In human high concentrations of GS can be found in astrocytes in brain tissue [3] and in perivenous parenchymal cells in the liver [2]. Loss of hepatic GS activity results in severe clinical conditions [4]. In particular, two mutations of human GS (R324C and R341C) were connected to congenital glutamine deficiency resulting in neonatal death [5]. In a single case known to date another GS mutation (R324S) was identified in a neurologically compromised patient [6]. However, the molecular mechanisms underlying the impairment of GS activity by these mutations have remained elusive.
In order to overcome this shortcoming, we applied molecular dynamics simulations, free energy calculations, and rigidity analyses. We show that all three mutations influence ATP binding, the first step of GS glutamine formation reaction [7]. In the case of the R324S and R324C mutants, we found a loss of direct salt-bridge interactions with the substrate ATP [7]. This likely hampers ATP binding, which deteriorates GS catalytic activity [5]. Remarkably, in the case of the R324S mutant, we observed water-mediated interactions with ATP [7] that reduce this effect and may explain the suggested higher GS residual activity [8]. Furthermore, we predicted the R341C mutant to result in a significant destabilization of helix H8, which should hamper glutamate binding. To further corroborate this suggestion, we introduced an additional GS variant through alanine mutagenesis of three amino acids that are located on helix H8 and interacting with R341, mimicking the loss of interactions in the R341C mutant. After GS overexpression in HEK293 cells, dot-blot analyses revealed that the structural stability of helix H8 was indeed impaired in the case of the newly introduced GS mutant [7]. This results in a loss of masking of the epitope in the glutamate binding pocket for a monoclonal anti-GS antibody by L-methionine-S-sulfoximine; in contrast, cells transfected with wild type GS did show the masking.
Our analyses reveal complex molecular effects underlying GS deactivation in three clinically relevant mutants [7]. Furthermore, since there is currently no adequate therapy available [8] to treat a glutamine deficiency caused by the R324S mutant, our findings could stimulate the development of ATP binding-enhancing molecules by which the R324S mutant can be “repaired”.

[1] Häussinger, D.: Eur. J. Biochem. 1983, 133(2):269-275.
[2] Häussinger, D.: Biochem. J. 1990, 267(2):281-290.
[3] Martinez-Hernandez, A. et al.: Science 1977, 195(4284): 1356-1358.
[4] Qvartskhava, N. et al.: P. Natl. Acad. Sci. USA 2015, 112(17): 5521-5526.
[5] Häberle, J. et al.: New. Engl. J. Med. 2005, 353(18): 1926-1933.
[6] Häberle, J. et al.: Mol. Genet. Metab. 2011, 103(1): 89-91.
[7] Frieg, B. et al.: PLoS Comput. Biol., 2016, DOI: 10.1371/journal.pcbi.1004693.
[8] Häberle, J. et al.: Orphanet J. Rare. Dis. 2012, 7(48): 1-10.

[BIO 5] A New Workflow for Creating Cellular, 3D-Models of the Human Brain on a Massively Parallel General Purpose Supercomputer

***H. Mohlberg**, B.Tweddell, T. Lippert, K. Amunts*

Digital models of individual brains are commonly used to provide a spatial reference system for human brain atlases [1]. They are indispensable to integrate data from different brains, sources, and modalities while considering the functionally relevant topography of the brain [2]. The spatial resolution of most of these digital atlases is in the range of millimeters. This limits

the integration of the information at the length scale of cortical layers, columns, microcircuits or cells. Therefore, we introduced the BigBrain data set with a resolution of 20µm isotropic as a new microstructural template for a human brain atlas. In addition, the BigBrain data set represents a tool to extract morphometric parameters of human brain organization. They serve as a "gold standard" for neuroimaging data obtained with a much lower resolution and thus can provide the necessary basis for realistic human brain models and simulation [3].
The generation of such BigBrain data sets is extremely time-consuming and labor-intensive. Based on the first BigBrain data set, we have created a second one to facilitate inter-subject variability analyses. The total size of about 7600 digitized histological sections with an in-plane resolution of 20µm amounts to about 0.6 TByte (using 16-bit gray value coding). Histological processing inevitably causes structural artifacts that have – in particular at the highest resolution – a significant impact on image processing. As a result, up to 40% of the sections demand time-consuming manual artifact corrections. The workflow for the 3D-reconstruction of this data set includes linear and nonlinear 2-dimensional alignment of histological sections at different scale levels to corresponding sections of the aligned MR-images, volume-to-volume registration of MR images to stacked histological sections, and section-to-section alignment of histological sections to each other or to MR images. This is carried out in an iterative manner. The process starts from a coarse 3D-reconstruction with images showing artifacts to a finer scale with images after their artifacts have been removed. Several iterations allow for consecutively improving the quality of the reconstructed data set. The continuous manual artifact correction of a couple of sections (about 100-200 per week) within a long period of time requested a dataflow management system that allows to automatically re-process only the subsequent data sets affected by the last modifications.
Due to the large amount of more than 500,000 data sets (e.g., original and multiple processed 2D and 3D data sets at different scale levels, linear and non-linear vector field files, log files for data provenance tracking) in combination with the complexity of the overall reconstruction workflow, the processing of BigBrain data sets requires advanced technology based on HPC for both data management and computing. The efficient data processing of a large amount of data sets in a complex reconstruction workflow using large numbers of compute nodes requires optimized distributed processing pipelines and parallelization. Data provenance tracking includes a detailed documentation of the processing steps and of the complex inter-dependencies of the data sets at each level of the multi-step reconstruction workflow. This is essential to restrict the re-computation to only those images that have to be re-processed, e.g. after improved manual repair, or newly implemented data processing steps. Successive computing algorithms were combined in one compute job to minimize costly I/O operations. Memory intensive programs, e.g. loading whole volumes for generating virtual sectioning planes, were parallelized with MPI. Python powered by mpi4py was used for programming processing pipelines and data provenance tracking tools. Computations were done on the HPC-cluster JUROPA and on its successor, JURECA, at the Jülich Supercomputing Centre, Germany. We have achieved a high throughput processing of thousands of images of histological sections in combination with sufficient flexibility, based on an effective, successive coarse-to-fine hierarchical processing. The workflow presented here in combination with the data provenance tracking tool was designed in order to process future whole brain image stacks with an even higher resolution of 1µm to open new perspectives for analyzing human brain organization at the microscopic level.

[1] Evans et al. (2012), ’Brain atlases and templates’, NeuroImage, vol. 62, no. 2, pp. 911-922
[2] Amunts et al. (2014), ’Interoperable atlases of the human brain’, NeuroImage, vol. 99, pp. 525-532
[3] Amunts et al. (2013), ‘BigBrain: An Ultrahigh-Resolution 3D Human Brain Model’, Science, vol. 340, no. 6139, pp. 1472-1475

[BIO 6] Mechanistic Study of ATP Cyclization as Catalyzed by Adenylyl Cyclase

***P. Vidossich**, S. van Keulen, U. Rothlisberger, J. Hellgren Kotaleski, P. Carloni*

Molecular simulation is expanding its scope to large and complex systems by synergetic use of molecular and mathematical modeling. In the context of neurobiology, systems biology approaches aim at reconstructing signaling networks in subcellular processes related to brain function. Molecular simulations can support the quantitative modeling of biochemical networks by characterizing molecular events involved in the network and estimating the associated kinetic parameters. Here we present an application of such approach, performed in the context of the EU flagship Human Brain Project (www.humanbrainproject.eu), to investigate a cascade of relevance for memory processes and which involves the enzyme adenylyl cyclase (AC). AC synthesizes cyclic adenosine monophosphate (cAMP), a second messenger involved in signaling cascade pathways. Activation of cAMP synthesis from ATP is triggered by the binding of G-protein subunit Gas•GTP to the AC enzyme. By means of hybrid QM/MM Car-Parrinello molecular dynamics simulations we investigated the enzymatic conversion from ATP to cAMP catalyzed by the C1•C2 interface of the heterodimeric AC5/2 in the presence of the activator Gas•GTP. The mechanical properties of the G-protein bound and unbound AC enzyme have also been compared in the attempt to rationalize how the G-protein modulates enzyme activity.

[BIO 7] Molecular View of Ligands Specificity for CAG Repeats in Anti-Huntington Therapy

***A. Bochicchio**, G. Rossetti, O. Tabarrini, S. Krauß, P. Carloni*

Huntington's disease is a fatal and devastating neurodegenerative genetic disorder for which there is currently no cure. The gene responsible for the disease encodes the Huntingtin protein (HTT), essential for brain development. The disease is caused by an expanded CAG repeat in the 5'-end of HTT, which encodes an abnormally long polyglutamine (polyQ) tract in the HTT protein. HD penetrance is related to the number n of CAG repeats. Mounting evidences are emerging that in addition to the polyQ protein also HTT mRNA transcripts with expanded CAG repeats (i) contribute to the pathogenesis of CAG disorders; (ii) aberrantly regulate several cellular mechanisms; (iii) bind to proteins in a repeat size-dependent manner to form pathological complexes. As recently shown by S.Krauß's laboratory, one of those involves the Midline-1 protein (MID1), in complex with protein phosphatase 2A (PP2A), which leads to an overproduction of aberrant HTT protein[1]. Inhibiting the formation of this pathological mRNA/proteins complex, targeting the expanded CAG mRNA transcript, can significantly reduce the HTT overproduction effect. Yet, the rational design of molecules specifically targeting the expanded CAG repeats is critically limited by the lack of structural information. We used well-tempered-based free energy calculations to investigate pose and affinity of the two ligands targeting CAG repeats for which affinities have been measured. These are the cation 4-guanidinophenyl 4-guanidinobenzoate (1) and 4-phenyl imidazole 4-1H-indole imidazole (2) (Kd=60(30) and Kd=700(80) nM, respectively)[2]. Our calculations, consistent with the experimental affinities, uncover the recognition pattern between ligands' and their RNA target. They also provide the molecular bases of their different specificity of the two ligands for CAG repeats. These findings pave the way for a structure-based hit-to-lead optimization to further improve ligand selectivity towards CAG repeat-containing mRNAs.

[1] Krauß, S.; Griesche, N.; Jastrzebska, E.; Chen, C., Translation of HTT mRNA with expanded CAG repeats is regulated by the MID1–PP2A protein complex. Nature 2013.
[2] Kumar, A.; Parkesh, R.; Sznajder, L. J.; Childs-Disney, J. L.; Sobczak, K.; Disney, M. D., Chemical correction of pre-mRNA splicing defects associated with sequestration of muscleblind-like 1 protein by expanded r(CAG)-containing transcripts. ACS Chem. Biol. 2012,

7 (3), 496-505.

[BIO 8] 3D Reconstruction of Nerve Fibers in the Vervet Monkey Brain

***O. Bücker**, A. Müller., A. Lührs., T. Dickscheid, S. Haas, M. Huysegoms, H. Spitzer, A.-M. Huynh, S. Köhnen, G. Tabbi, P. Schlömer, M. Schober, N. Schubert, H. Wiese, M. Axer*

The main goal of our project is the generation of a high-resolution, large-scale, virtual nerve fiber model of vervet monkey brain to be assembled from 1,200 serial images of histological brain sections [1]. This means, the project is purely data driven. The fundamental imaging data were acquired by means of polarized light imaging (3D-PLI), a neuroimaging microscopic technique that utilizes the optical birefringence of brain tissue to visualize nerve fibers, fiber tracts and their spatial orientations at microscopic resolutions [2,3]. In order to build a 3D fiber model of a brain, a complex image analysis and processing workflow has to be applied, comprising image segmentation, stitching, blind source separation, birefringent signal interpretation, and image registration. Considering the pure size of the targeted data set (Terabyte range), it is evident that a high performance computing solution is required to produce the unique data set in a reasonable time frame. JURECA is the supercomputer and UNICORE the framework of choice to carry out the data analysis in an efficient and automatized way.
In first three months of the project, we focused at adopting our analysis workflow to requirements set by JURECA, since most of the in-house developed software packages included were implemented and optimized for efficient use at the (now de-installed) JUDGE GPU cluster [4]. We will introduce the concept of our workflow-based nerve fiber reconstruction and report on our experience with both supercomputing systems.

[1] Zilles K, Palomero-Gallagher N, Gräßel D, Schlömer P, Cremer M, Woods R, Amunts K, Axer M (2016) High-resolution fiber and fiber tract imaging using polarized light microscopy in the human, monkey, rat and mouse brain. In: Axons and brain architecture (Rockland, ed.), pp 369-39: Elsevier Academic Press.
[2] Axer M, Amunts K, Gräßel D, Palm C, Dammers J, Axer H, Pietrzyk U, Zilles K (2011) A novel approach to the human connectome: Ultra-high resolution mapping of fiber tracts in the brain. NeuroImage 54:1091-1101.
[3] Axer M, Gräßel D, Kleiner M, Dammers J, Dickscheid T, Reckfort J, Hütz T, Eiben B, Pietrzyk U, Zilles K, Amunts K (2011) High-Resolution Fiber Tract Reconstruction in the Human Brain by Means of Three-Dimensional Polarized Light Imaging. Frontiers in Neuroinformatics 5:1-13.

[BIO 9] Computational Study of Copper (II) Binding to the Physiological Form of Alpha-Synuclein

***E. Abad**, F. Musiani, D. Dibenedetto, G. Rossetti, A. Binolfi, C. Fernández, P. Carloni*

Intrinsically disorder proteins (IDPs) defy the classic structure-function paradigm. They are important for a wide variety of processes in eukaryotes, from signaling to protein biosynthesis. Some prevalent diseases, such as Alzheimer and Parkinson's disease are related to IDP malfunctioning; and others, such as Creutzfeldt–Jakob disease, involve proteins with unstructured regions. Alpha-synuclein (AS) is an IDP expressed in the nervous system, that is thought to be a modulator of synaptic transmission, and it is the primary component of amyloid fibrils (Lewy bodies) found in patients with Parkinson's disease [1]. Recently it has been discovered that it is acetylated in vivo [2].
Copper ions have shown to be important aggregation modulators. Cu(II) binding to the acetylated physiological form of AS (AcAS) has been shown to be different from its non-

acetylated counterpart [3,4]. In particular, experiments show that the highest affinity binding site of AcAS is at the 48VVHGV52 sequence [3]; while in non-acetylated AS it is on 1MD2 [4]. In the present study, we use computational methods to investigate the effect on structural determinants on AS acetylation and Cu(II)-binding to AcAS. Three possible Cu(II) binding geometries, suggested by EPR and NMR spectroscopic measurements [5,6] are considered. Due to the lack of permanent secondary structure of IDPs, we are using computational techniques designed to accelerate the exploration of the conformational space such as replica exchange molecular dynamics in its most recent implementation (REST2) [7]. Force field parameters for the Cu(II) ion are being developed using the so-called Force Matching procedure as in refs [8]. Spectroscopic calculations of AS, AcAS and Cu(II)-AcAS are compared with experimental values in order to assess the predictive power of our calculations [9].

[1] L. Stefanis (2012) Cold Spring Harb. Perspect. Med. 2(2), a009399
[2] B. Favuet, et al. (2012) J. Biol. Chem. 287, 28243
[3] G. M. Moriarty, C. A. S. A. Minetti, D. P. Remeta, J. Baum (2014) Biochemistry 53, 2815
[4] A. Binolfi et al. (2010) Inorg. Chem. 49, 10668
[5] R. M. Rasia et al. (2005) Proc. Natl. Acad. Sci. 102, 4294
[6] D. Valensin et al. (2011) Metallomics 3, 292
[7] L. Wang, R. A. Friesner, B. J. Berne (2011) J. Phys. Chem. B 115, 9431
[8] T. H. Ngyen et al. (2014) J. Chem. Theory Comput. 10, 3578
[9] G. Rossetti, F. Musiani, E. Abad, D. Dibenedetto, H. Mouhib, C. O. Fernandez, P. Carloni. Phys. Chem. Chem. Phys. (2016). In press. DOI: 10.1039/C5CP04549E

[BIO 10] Self-Propelled Rods with Density-Dependent Motility

***C. Abaurrea Velasco**, M. Abkenar, K. Marx, T. Auth, G. Gompper*

The collective behavior of microswimmers has gained considerable attention in the recent years [1]. Examples of microswimmers span from biological cells and bacteria to human-made nano-robots. Here, we propose a model for self-propelled rods in two dimensions that interact with a soft repulsive potential and have a density-dependent propelling force. We model each rod by a number of beads to calculate the rod-rod interactions. The soft repulsive potential allows rods to cross each other, making our system suitable for modeling quasi-2D experiments [2]. In actin or microtubule motility assays, cytoskeletal filaments swim on top of motor proteins that are anchored to a planar substrate. The motors propel the filaments, creating an out-of- equilibrium quasi-2D system. If the local density of filaments is bigger that the density of motors, motor sharing occurs. When two rods cross or become close to each other, their propelling forces decrease. This is caused by the fact that there are less motors attached to each of the rods, we call this phenomenon motor sharing [3]. Inspired by the collective phenomena observed in actin-motility assays, we systematically examine the phase behavior of rods with density-dependent propelling forces. Rod density, propelling force and motor sharing give rise to rich phase diagrams, where we observe that motor sharing induces cluster formation. We predict that smaller motor densities lead to more stable clusters.

[1] J. Elgeti, R. Winkler, and G. Gompper, Rep. Prog. Phys. 78, 5 (2014).
[2] M. Abkenar, K. Marx, T. Auth, and G. Gompper, Phys. Rev. E 88, 062314 (2013).
[3] F. Farrell, M. Marchetti, D. Marenduzzo, and J. Tailleur, Phys. Rev. Lett. 108, 248101 (2012).

[BIO 11] Ligand Recognition and Substrate Coupling in Glutamate Transporters

***C. Alleva**, C. Fahlke, J.-P. Machtens*

Excitatory amino acids transporters (EAATs) guarantee the signal termination in the central nervous system, uptaking glutamate from the synaptic cleft into astrocytes and glial cells. Glutamate is the major excitatory neurotransmitter and an impairment of its transport can lead to neurological disorders. EAATs are secondary active transporters with a complex transport stochiometry involving three sodium ions, one potassium ion and one proton, which grants concentrative uptake of the transmitter against a millionfold concentration gradient.
In recent years, X-ray structures of the prokaryotic homolog GltPh in multiple conformations have significantly advanced our understanding of the EAAT transport mechanism. However, it is still not fully resolved how EAATs recognize and bind their substrates to achieve highly selective and efficient transport at the same time. In addition, it is only partially understood how EAATs couple substrate uptake to the cotransport of three Na+ ions, with only two out of three Na+ binding sites reliably identified to date.
We here conducted all-atom molecular dynamics simulations of GltPh, with a particular focus on the role of the third Na+ site in the substrate coupling. During our simulations, occupation of the putative third sodium site secured the substrate in the locked binding pocket. The rearrangement of the side chain of methionine in position 311, induced by the sodium residence, stabilizes the tightly bound conformation due to the release of sterical clashes with the closed hairpin 2 - the extracellular gate to the substrate binding site - that in turn ensures a tight seal of the substrate binding pocket.
A deeper knowledge of these dynamics an of the role of the sodium coupling is expected to heltp to resolve the transport mechanisms of EAATs and to understand dysfunctions of these proteins in pathological conditions.

[BIO 12] Lipid Transport by the ABC Transporter MDR3

***M. Bonus**, H. Gohlke*

Hepatocytes regulate the directional transport of endogenous substances and xenobiotics through a variety of membrane transporters in the sinusoidal and canalicular membrane [1]. Among other important exporters, the canalicular membrane contains the ATP binding cassette (ABC) transporter multidrug resistance protein 1 (MDR1, ABCB1, P-glycoprotein) and the homologous multidrug resistance protein 3 (MDR3, ABCB4). Despite their high sequence similarity of 86 %, MDR1 and MDR3 differ greatly regarding tissue expression and function [2,3]. While MDR1 is ubiquitously expressed and transports a variety of structurally unrelated compounds including drugs, lipids, and peptides, MDR3 is almost exclusively found in the canalicular membrane of hepatocytes and is a floppase specific for phosphatidylcholine lipids [4]. However, the structural basis for this divergent specificity has remained elusive so far as most residues in the drug-binding cavity of MDR1 are identical in MDR3.
Based on molecular dynamics (MD) simulations, we present evidence that the mechanism of substrate translocation in MDR3 may be different from the classical cavity-mediated transport in MDR1: In all five MD simulations of membrane-embedded MDR1, we observed penetration of two lipids into the cavity of the transporter, mediated by two entry gates formed by its transmembrane helices; this is in stark contrast to the simulations of MDR3, in which lipid access to the cavity of MDR3 was significantly hampered and only observed for one lipid in two out of five simulations. The latter results from transmembrane helices that form the entry gates in MDR3 adopting a different, kinked conformation early in the simulations, which restricts the access of lipids by narrowing the penetrable space. Our simulations indicate that MDR3 does not utilize a dedicated lipid binding cavity for the translocation of phosphatidylcholine lipids. In light of the recently solved crystal structures of the Ca^{2+}-dependent phospholipid scramblase TMEM16 [5] and the lipid-linked oligosaccharide flippase

PglK [6], which suggest that lipid flipping occurs on the protein surface rather than in the central substrate cavity, we hypothesize that this mechanism for lipid transport is also valid for MDR3.
We consider our simulations as a framework for further *in silico* and *in vitro* studies to validate the proposed mechanism. In particular, we aim at computing free energy profiles of lipid transport along different translocation pathways and, in collaboration, transform MDR3 into an MDR1-like multidrug transporter by site-directed mutagenesis. Eventually, these results could contribute to a better general understanding of the structure-function relationship of ABC transporters.

[1] Nicolaou, M. et al. Canalicular ABC transporters and liver disease. J. Pathol. 226 (2012), 300-315.
[2] van der Bliek, A. M., Kooiman, P. M., Schneider, C. & Borst, P. Sequence of mdr3 cDNA encoding a human P-glycoprotein. Gene 71 (1988), 401-411.
[3] Smit, J. J. et al. Tissue distribution of the human MDR3 P-glycoprotein. Lab. Invest. 71 (1994), 638-649.
[4] van Helvoort, A. et al. MDR1 P-glycoprotein is a lipid translocase of broad specificity, while MDR3 P-glycoprotein specifically translocates phosphatidylcholine. Cell 87 (1996), 507-517.
[5] Brunner, J. D., Lim, N. K., Schenck, S., Duerst, A. & Dutzler, R. X-ray structure of a calcium-activated TMEM16 lipid scramblase. Nature 516 (2014), 207-212.
[6] Perez, C. et al. Structure and mechanism of an active lipid-linked oligosaccharide flippase. Nature (2015), 433-438.

[BIO 13] Revealing the Structural Properties of p-DTS(FBTTh2)2 with the Help of MD-Simulations

***A. Bourdick**, S. Gekle*

With the advent of organic photovoltaics promising materials for organic solar cells have become a strong focus of research. One particular interesting manufacture strategy is the push-pull chromophore design, whereby an electron rich donor unit and an electron deficient acceptor unit are placed alternating on the same molecule [1,2]. With the help of MD-Simulations we investigate the system p-DTS(FBTTh2)2, which is a promising candidate of the push-pull design for future usage in commercial organic solar cells. In particular we are interested in the structure and conformation of aggregated states in different solvents, and various physical properties, like the free energy of the system in dependence of the distance between molecules.
The results for this system are presented in this poster to demonstrate the possibilities of what we can achieve with the computing power of the Jülich Supercomputing Centre. Furthermore, we give an outlook into similar research topics we want to investigate in the future, for example related systems.

[1] Gendron, D.; Leclerc, M. New Conjugated Polymers for Plastic Solar Cells. Energy Environ. Sci. 2011, 4, 1225-1237.
[2] Duan, C.; Huang, F.; Cao, Y. Recent Development of Push-Pull Conjugated Polymers for Bulk- Heterojunction Photovoltaics: Rational Design and Fine Tailoring of Molecular Structures. J. Mater. Chem. 2012, 22, 10416-10434.

[BIO 14] Binding of the Antagonist Caffeine to the Human Adenosine Receptor hA2AR in Nearly Physiological Conditions

***R. Cao**, G. Rossetti, P. Carloni, A. Bauer*

Lipid composition may significantly affect membrane proteins function, yet its impact on the protein structural determinants is not well understood. Here we present a comparative molecular dynamics (MD) study of the human adenosine receptor type 2A (hA2AR) in complex with caffeine - a system of high neuro-pharmacological relevance - within different membrane types. These are POPC, mixed POPC/POPE and cholesterol-rich membranes. 0.8- μs MD simulations unambiguously show that the helical folding of the amphipathic helix 8 depends on membrane contents. Most importantly, the distinct cholesterol binding into the cleft between helix 1 and 2 stabilizes a specific caffeine-binding pose against others visited during the simulation. Hence, cholesterol presence (~33%-50% in synaptic membrane in central nervous system), often neglected in X-ray determination of membrane proteins, affects the population of the ligand binding poses. We conclude that including a correct description of neuronal membranes may be very important for computer-aided design of ligands targeting hA2AR and possibly other GPCRs.

[BIO 15] Prediction of Ligand-Protein Binding and Unbinding Kinetic Data for Neural Signaling Cascades

***R. Casasnovas Perera**, P. Tiwary, V. Limongelli, M. Parrinello, P. Carloni*

At a molecular level neural function consists of intricate signalling pathways. The dynamics and outcome of such pathways can be predicted by Systems Biology methods that use the rate constants of the chemical and physical events that constitute the pathway. Kinetic constants are often difficult to access from experiment due to the fast nature of the events. In other cases it is only possible to obtain pseudo-kinetic or apparent kinetic constants of reactions that occur in multiple linked steps. Additionally, it is extremely difficult to obtain experimental structural information of the transition states due to their short lifetime. We use molecular dynamics (MD) simulations to calculate the kinetics of protein-ligand binding and unbinding (kon and koff). At a structural level, MD simulations provide a description the process with atomic resolution. More importantly, MD simulations are required to describe rigorously the protein and ligand flexibility as well as the solvent, which are crucial factors for the binding and unbinding processes.

Protein-ligand binding events typically occur in a timescale that spans from milliseconds to hours. Nowadays the computational costs of atomistic MD only allow simulations of events taking place in microsenconds. Therefore ligand-binding/unbinding is beyond the capabilities of standard MD methods. We overcome this limitation by using Metadynamics simulations, a statistical mechanics technique by which a slow event (i.e. protein ligand binding and unbinding) is accelerated so that it takes place within the timescale accessible for MD simulations [1]. The key point is that the acceleration takes place in a controlled way so that the real characteristic time and kinetic constant of the event can be easily recovered [2].

Here we apply this approach to predict binding and unbinding kinetic constants of inhibitors of p38 MAP kinase, an enzyme activated by stress signals that particiaptes in the molecular development of Alzheimer's disease and Amyotrophic Lateral Sclerosis [3-6]. These are derivatives of the so-called BIRB 796 molecule, which entered Phase II human clinical trials for the treatment of autoimmune disorders. We anticipate that the application of this test case will pave the way for a variety of unprecedented applications in the study of signalling cascades and ligand design.

[1] Barducci, A.; Bussi, G.; Parrinello, M. Phys. Rev. Lett. 2008, 100, 020603.
[2] Tiwary, P.; Parrinello, M. Phys. Rev. Lett. 2013, 111, 230602.

[3] Chang, K.; De Pablo, Y.; Lee, H.; Lee, H.; Smith, M. A.; Shah, K. J. Neurochem 2010, 113, 1221.
[4] Ferrer, I.; Gomez-Isla, T.; Puig, B.; Freixes, M.; Ribé, E.; Dalfó, E.; Avila, J. Curr. Alzheimer Res.2005, 2, 3.
[5] Ackerley, S.; Thornhill, P.; Grierson, A. J.; Brownlees, J.; Anderton, B. H.; Leigh, P. N.; Shaw, C. E.; Miller, C. C. J. Cell Biol., 2003, 12, 489.
[6] Tortarolo, M.; Veglianese, P.; Calvaresi, N.; Botturi, A.; Rossi, C.; Giorgini, A.; Migheli, A.; Bendotti, C. Mol. Cell. Neuroscience, 2003, 23, 180.

[BIO 16] Potential of Mean Force Calculations Predict a Stable Conformational Intermediate in the Mechanism of Pyruvate Phosphate Dikinase (PPDK)

***D. B. Ciupka**, A. Minges, G. Groth, H. Gohlke*

Pyruvate phosphate dikinase's (PPDK) critical role in the energy metabolism of C4 plants and parasites combined with its absence in humans makes this protein an interesting target for the development of C4 plant-specific herbicides and antiparasitic drugs. The reaction mechanism of PPDK involves a large-scale swivelling motion of the central domain (CD) that shuttles a phosphoryl group over a distance of ~45 Å between two reactions centres, placed at the nucleotide-binding domain (NBD) and the PEP / pyruvate-binding domain (PBD). The swivelling motion model is substantiated by several static X-ray crystal structures showing two extreme conformations of the CD as well as open and closed conformations of the NBD. However, investigations of the intramolecular processes that explain and connect the conformational dynamics to functional relevance have remained elusive so far.
Here, we provide insights into the dynamics and energetics of the swivelling motion of the CD and the opening / closing motion of the NBD aiming at resolving the mechanism of PPDK at atomic resolution. We predicted a stable conformational intermediate of the CD during the swivelling motion by umbrella sampling / potential of mean force (PMF) calculations, which was corroborated by unrestrained molecular dynamics (MD) simulations. A recent X-ray structure of PPDK from *Flaveria pringlei* confirmed our predictions. Furthermore, our PMF results reveal an energetic preference for a coordinated movement of the CD with the opening / closing motion of the NBD, which is also supported by cross-correlations found between these motions from all available X-ray structures as well of from structures obtained by multiple MD simulations of an aggregate length of ~5 µs. Finally, our PMF results suggest that the phosphorylation state of the CD influences the preferred direction of motion of this domain between NBD and PBD, in agreement with the proposed catalytic mechanism. Together, our results may explain how PPDK functions efficiently despite the required large-scale transfer of a phosphoryl group during catalysis and can open up a route for the development of (allosteric) PPDK inhibitors.

[BIO 17] Swimming and Swarming of E. coli Bacteria

*J. Hu, **T. Eisenstecken**, G. Gompper, R. G. Winkler*

Locomotion is a major achievement of biological evolution. Microorganisms, such as bacteria, algae, and sperm cells are equipped with flagella and are able to exploit drag for their propulsion. Thereby, many bacteria utilize rotating flagella. We developed a mechano-elastic model for a bacterium, where a spherocylindrical body is propelled by rotating helical flagella. To take hydrodynamic interactions into account, the bacterium model is coupled to the Multiparticle Collision Dynamics algorithm, a mesoscale hydrodynamic simulation technique. We find that the hydrodynamic friction coefficients of the bacterium show qualitative agreement with experimental results of E. coli. The measured flow field shows a force-dipole-like pattern in the swimming plane and two vortices perpendicular to its swimming direction

arising from counter-rotation of the cell body and the flagella. We investigate the near-surface swimming behavior and find that the cell is sensitive to nanoscale changes in the surface slip length. Furthermore, we discuss briefly collective behavior of bacteria.

[BIO 18] Mechanical Property Based Sorting of Red Blood Cells in Deterministic Lateral Displacement Devices

E. Henry, *S. H. Holm, Z. Zhang , J. P. Beech, J. O. Tegenfeldt, D. A. Fedosov, G. Gompper*

The use of deterministic lateral displacement (DLD) devices for sorting biological particles based on their mechanical and conformational properties has received significant interest from teams attempting to diagnose disease from blood. We investigate red blood cell (RBC) sorting under various DLD geometries and probe device sensitivity to the mechanical properties of RBCs. Mesoscale hydrodynamic simulations are employed to probe RBC transit dependency on properties such as viscosity contrast and membrane elasticity. Results indicate that RBC dynamics are important for determining whether or not RBCs travel in a displacement or zigzag mode: tank treading and the associated lift force are attributed with displacement motion whereas tumbling appears to encourage zigzagging through obstacle arrays. Simulations achieve quantitative agreement with trajectories obtained from experimental DLD set-ups and a viscosity based sorting scheme is tested based on the simulated findings.

[BIO 19] The von Willebrand Factor Conformation in Blood Flow

M. Hoore*, K. Müller, D. A. Fedosov, G. Gompper*

The von Willebrand factor (VWF) is the largest soluble concatemer of VWF protein dimers in blood [1, 2] which plays an important role in primary haemostasis. Normally, VWF polymer is in a globular form and intangible for adhesive GPIbα or other adhesive receptors. In case of an injury, VWF A3-domain adheres to the collagens [3, 2] exposed at the injured endothelium and stretches due to elongational forces exerted on the chain. When stretched, the polymer exposes its ligands to platelet GPIbα receptors and initiates haemostasis. The positioning and conformation of VWFs in blood flow are very important for regulating haemostasis. In order to study VFW behavior in blood flow, we use the Smoothed Dissipative Particle Dynamics as a mesoscale simulation method [4] for solvents. For RBCs, the multiscale coarse-grained red blood cell model [5, 6] is considered. Accordingly, we have studied ultra large VWF polymers conformation and their positioning in the cross section of blood flow by using coarse-grained attractive bead model for VWF polymers which is capable to represent VWF critical shear dependent stretching [7, 8]. We observe that the ultra large VWF polymers, similar to platelets and other microscale blood components, are pushed into an RBC free layer near the vessel wall. This phenomenon, known as margination [9, 10], is beneficial for haemostasis by increasing adhesion probability of VWF and platelets at the wall. Moreover, the marginated polymers feel stronger elongational forces in the RBC free layer compared with the polymers at the center of the vessel, resulting in easier polymer stretching and more efficient haemostasis at the vessel wall.

[1] De Ceunynck, K. et al. Blood 121(2):(2013) 270–277.
[2] Springer, T.A. Blood 124(9):(2014) 1412–1425.
[3] Nishida, N. et al. Nat Struct Mol Biol 10(1):(2003) 53–58.
[4] Espanol, P. and Revenga, M. Phys Rev E 67(2):(2003) 026705.
[5] Fedosov, D.A. et al. Comput Method Appl M 199(29):(2010) 1937–1948.
[6] Fedosov, D.A. et al. Biophys J 98(10):(2010) 2215–2225.
[7] Alexander-Katz, A. et al. Phys Rev Lett 97:(2006) 138101.

[8] Schneider, S. et al. P Natl Acad Sci USA 104(19):(2007) 7899–7903.
[9] Reininger, A. Haemophilia 14(s5):(2008) 11–26. [10] Müller, K. et al. J Comput Phys 281: (2015) 301–315.

[BIO 20] Towards QSAR Modelling for Prion Therapeutics

***M. J. Huang**, G. Rossetti, M. De Vivo, P. Carloni, G. Legname*

Prion diseases are a group of infectious fatal neurodegenerative disorders [1]. The deposits of the self-replicating β-rich isoform prion protein (PrPSc) converted from its cellular form (PrPC) are considered to be central events in the course of the disease [1]. To understand the prion pathogenesis, achieve early diagnosis, prophylactic and effective treatment, several scaffolds of chemical compounds have been developed. These compounds may interact with either PrPC or to PrPSc, thus increasing PrPC stability or PrPSc clearance. Some achieve anti-prion activities through specific binding. Several binding sites have been suggested but the knowledge of mode-of-actions is scarce. Up-to-date, there are no effective therapeutics.
Recent structure deposits (PDB 4MA7, 4MA8[2]) have revealed binding information of tricyclic ligands (Promazine and Chloropromazine) in complex with mouse PrP. Tricyclic derivatives are considered GN8 [3] fused ring derivatives. GN8 is believed to achieve its anti-prion activity by specific binding [3]. The binding site of Promazine derivatives in moPrP is in agreement to docking molecular dynamics NMR studies of GN8[2]. Altogether, it seems some prion recognition motifs (of GN8 derivatives and 2-3 fused ring analogs) specifically interact with the shallow cavity formed between β1,2 and α2. The particular importance of this region for mediating the PrPC-PrPSc conversion was later elegantly illustrated by the introduction of new β0 (residues 118-122) from the HuPrP(23-231)·Nb484 crystal complex (PDB 4KML)[4]. Collectively, these studies provide a rationale for investigating the interactions between anti-prion compounds and the shallow cavity in the mechanism of PrPC-PrPSc conversion. We conducted a brief quantitative structure-activity relationship (QSAR) study to extract binding information from published data using statistical calculations.
Based on the assumption that anti-prion compounds derived from GN8 share similar binding specificity, an anti-prion compound database has been curated from literature for QSAR study. As the structure-based methods gain its dominance, the value of statistically based QSAR approaches raises in helping to guide lead optimization[5]. This database contains ca. 200 compounds with known anti-prion activities (IC50) and can be subdivided into 5 dataset by the type of cell line and the incubation time of inhibitors. 1, 2 & 3D descriptors have been generated. Generated descriptors values were coherent to ligands included in the database and a QSAR model for each dataset has been built using ANOVA statistical method. The results show that a certain degree of flexibility and aromatic moiety is beneficial to the activity. However, the activity drops when the ligand is full of aromatic rings in some sets.

[1] Prusiner, S. et al. (2013) Editorial (Thematic Issue: Recent Advances of Biology and Medicinal Chemistry of Prion Protein and Prions: On the Road to Therapeutics). Curr. Top. Med. Chem. 13, 2395–2396
[2] Baral, P.K. et al. (2014) Structural basis of prion inhibition by phenothiazine compounds. Structure 22, 291–303
[3] Kuwata, K. et al. (2007) Hot spots in prion protein for pathogenic conversion. Proc. Natl. Acad. Sci. 104, 11921–11926
[4] Abskharon, R.N.N. et al. (2014) Probing the N-terminal β-sheet conversion in the crystal structure of the human prion protein bound to a nanobody. J. Am. Chem. Soc. 136, 937–44
[5] Cherkasov, A. et al. QSAR modeling: Where have you been? Where are you going to?, Journal of Medicinal Chemistry, 57. (2014) , 4977–5010

[BIO 21] How the HPA-1 Polymorphism Affects Structure and Dynamics of Integrin αIIbβ3

***G. Pagani**, J. P. Ventura Pereira, N. Homeyer, V. R. Stoldt, R. E. Scharf, H. Gohlke*

The human platelet antigen (HPA)-1 alloimmune system is a biallelic system carried by the megakariocyte/platelet specific integrin αIIbβ3, which mediates platelet adhesion and aggregation; it is essential for hemostasis but can also foster thrombus formation. The HPA1 polymorphism of αIIbβ3 results from a leucine-to-proline exchange at residue 33 of the mature β3 subunit. Consequently, the HPA-1 pattern can be expressed as either HPA-1a (Leu33) or its variant isoform HPA-1b (Pro33) [1]. This mutation is highly relevant from a clinical perspective as patients with coronary artery disease who carry the HPA-1b allele experience their myocardial infarction 5.2 years earlier than HPA-1a/1a patients [2]. As such, HPA-1b is believed to be a prothrombotic variant of αIIbβ3 integrin, characterized by increased adhesion, increased thrombus stability, and increased outside-in signaling. However, the underlying mechanism through which this mutation, located more than 90 Å away from any of the binding sites, contributes to the heightened activatability of the integrin has, so far, still remained elusive. In the present study, a combined strategy, integrating large-scale all-atom MD simulations with FRET measurements, was used to characterize the nature of this phenotype at an atomic level. In detail, the ectodomains of the two αIIbβ3 variants in the closed conformation were used as model systems, and molecular dynamics (MD) simulations of in total 6 μs length were carried out to investigate the consequences of the Leu33Pro substitution on the structure and dynamics of αIIbβ3. In parallel to the MD simulations, transfected and fluorescently tagged HEK293 cells stably expressing either Leu33 or Pro33 were generated, and FRET measurements were applied to explore conformational changes occurring in the cytoplasmic tails upon integrin activation. Comparative analyses of the MD trajectories reveal how the Leu33Pro mutation disrupts the inter-domain interface at the genu of integrin and how this destabilization percolates across the entire structure, thus leading to the system being more easily activatable. The increased tendency to get activated in the presence of Pro33 is experimentally validated by FRET measurements, indicating a more extended spatial separation (>100 Å) of the cytoplasmic tails in Pro33 than in Leu33 cell clones ($p = 0.003$). Together, these findings explain how a single point, distant mutation can allosterically influence the fine-tuned conformational equilibrium of integrin αIIbβ3.

[1] Kunich, T.J., Newman, P.J., Blood, 1992, 80, 1386-1404.
[2] Scharf R.E. et al., J. Thromb. Haemost., 2005, 3, 1522-1593.

[BIO 22] Structural Determinants of the mitoNEET Protein in Solution from Molecular Simulation

***L. Pesce**, O. Faust, V. Calandrini, G. Rossetti, S. Tamir, A. Friedler, A. Bauer, R. Nechushtai, P. Carloni*

Parkinson's disease (PD) is currently a neurodegenerative disease affecting about 1% of the population over the age of 65. The discovery of new effective potential therapeutic targets for this and other neurodegenerative diseases is thus of paramount importance. Recently, proteins belonging to the NEET family (mitoNEET, mNT and NAF-1) are emerging as potential new targets[1].
The NEET proteins are homo dimeric iron-sulfur proteins, characterized by a β-cap and the CDGSH domain. The latter is a 16 amino acids long domain, which is the harbour of the 2Fe-2S cluster[2]. The c-terminal of each monomer of mNT is a transmembrane helix bounded to the outer mitochondrial membrane (OMM).
Although the pathways of the NEET proteins are not fully understood, this protein has been demonstrated to be determinant in the heme homeostasis and in the regulation of the reactive

oxygen species (ROS)[2].
In the first part of my research I modelled the soluble domain of the mNT (pdbID: 3EW0[3]) protein by using a combination of *ab initio* and classical molecular dynamics (MD). In order to get the parameters required to the classical MD, I applied the Seminario's method on the 2Fe-2S cluster binding domain[4].
Our computational model nicely reproduce the structural experimental data and a comparison with spectroscopic data is also proposed.
In the second step of my research, computational models will be used to implement receptor-based virtual screening of novel potential compound to be tested experimentally (Prof. Bauer INM-2). The constant iteration between the simulations and experiments will secure a continuous improvement of the original ligands/drugs set.

[1] Kundal RK. and Sharma SS., Peroxisome proliferator-activated receptor gamma agonists as neuroprotective agents, Drug News Perspect 23 (2010), 241-256.
[2] Tamir S. et al., Structure-function analysis of NEET proteins uncovers their role as key regulators of iron and ROS homeostasis in health and disease, Biochim Biophys Acta 1853 (2015), 1294-1315.
[3] Paddock, ML., et. al., MitoNEET is a uniquely folded 2Fe–2S outer mitochondrial membrane protein stabilized by pioglitazone, Proc. Natl Acad. Sci. USA 104 (2007), 14342–14347.
[4] Carvalho ATP. et Al., Parameters for molecular dinamics simulation of iron-sulfur proteins, J Comput Chem 34 (2013), 1540-1548.

[BIO 23] An Additional Ligand Binding Site in the TAS2R46 Bitter Taste Receptor

***M. Sandal**, M. Behrens, A. Brockhoff, F. Musiani, A. Giorgetti, P. Carloni, W. Meyerhof*

Most human G protein coupled receptors (GPCRs) are activated by small molecules binding to their 7-transmembrane (7-TM) helix bundle. These receptors belong to basally diverging branches: the 25 bitter taste 2 receptors and most members of the very large rhodopsin-like/class A GPCRs subfamily. Some members of the latter branch have been suggested to feature not only an orthosteric agonist-binding cavity but also a vestibular cavity, involved in the binding process. Here we present a hybrid molecular mechanics/coarse-grained (MM/CG) molecular dynamics approach on a widely studied bitter taste receptor (TAS2R46) receptor, in complex with its natural agonist strychnine. Molecular simulations find two cavities hosting the agonist, which together elucidate experimental data. This mechanism shares similarities with the one suggested for the evolutionarily distant class A GPCRs. It might be instrumental for the remarkably broad but specific spectrum of agonists of these chemosensory receptors.

[BIO 24] The Flexibility of His516 Negatively Impacts the Catalytic Activity of Glucose Oxidase

*D. Petrović, R. Ostafe, R. Fischer, **B. Strodel***

The catalytic ability of an enzyme originates from the stabilization of a transition state geometry for a ligand conversion. Catalytic groups, in complex with a ligand, lower the activation energy for a chemical transformation. The preorganization of the active site is among the key elements for enhanced catalysis. The relative residue rigidity is often higher for the catalytic than for the non-catalytic amino acids. We examined two new crystal structures of the highly active glucose oxidase (GOx) mutants in order to identify the cause of the increased catalytic potency. The His516 residue in the wt-GOx active site has a very flexible side chain. Its flexibility negatively impacts the catalytic activity by making the active site geometrically less suitable for the concerted proton and hydride transfer. The molecular

dynamics analysis supplements the crystallographic data, showing that His516 stays more rigid in the mutants. The comparative free energy surface analysis as a function of the His516 side chain dihedral angles χ1 and χ2 shows the presence of one free energy minimum in the mutant GOx. However, the wild-type enzyme is characterized by two distinct minima. The mutant possesses the stiffest active site with the optimal geometry for glucose interconversion to gluconolactone. We conclude that the antiperiplanar arrangement of His516 is catalytically active while the synclinal conformation is catalytically inactive, or it contributes to catalysis only negligibly.

[BIO 25] Multiscale Simulations of Odorant Receptors

F. Fierro *, T. Tarenzi , V. Calandrini , A. Giorgetti, P. Carloni*

Olfactory receptors (ORs) allow the discrimination among more than 1 trillion different olfactory stimuli: one odorant can activate numerous types of ORs, while a single OR can be activated by several different odorants. These data clearly underlie the crucial role of the sense of smell during evolution. ORs belong to the largest membrane-bound G-protein-coupled receptors (GPCRs) superfamily expressed by mammals. Unfortunately, experimental structural information on ORs is lacking. Here we are applying hybrid molecular mechanics/coarse grained simulations (Leguèbe et al., PLoS ONE 7(10): e47332 (2012)) to investigate the receptor OR7D4. The approach has shown to give reliable structural predictions for a variety of other GPCRs for which structural information is not available (Biarnés et al., PLoS ONE 5(8): e12394 (2010), Sandal et al., J. Chem. Theory Comput. 11(9): 4439–4449 (2015)). Our final goal is to predict the agonists binding mode in the receptor and the effect of mutations that affect odor perception.

Miscellaneous Engeneering

[SE 1] Size, Shape and Spectral Analysis of Nanoparticles by Analytical Ultra-centrifugation Using UltraScan

***J. Walter**, W. Peukert*

Analytical Ultracentrifugation (AUC) is a powerful and versatile tool to determine the size, shape and density of macromolecules and particles directly in solution based on their sedimentation properties. Even complex mixtures can be addressed because the measured signals of individual species are not superimposed as it is the case in ensemble-based scattering experiments. Data evaluation is achieved using sophisticated software packages like UltraScan3 which makes use of direct boundary models and HPC. The sedimentation profiles are fitted to adaptive space-time finite element solutions[1] of the Lamm equation considering the sedimentation and diffusion transport in the AUC[2]. AUC equipped with a custom made multiwavelength extinction detector (MWL-AUC) detects wavelengths reaching from 230 to 1100 nm simultaneously instead of just one which is provided by the commercial AUC. Thus, the informational content of the MWL-AUC is much higher as the wavelength dimension is added. However, such data requires HPC resources as a desktop PC would need about 40 hours for analyzing a single MWL data set. In a standard experiment four samples are measured simultaneously and two experiments can be conducted per day. Hence, only with HPC it is possible to evaluate the data generated via MWL-AUC.
In our poster the possibilities of nanoparticle (NP) analysis using direct boundary modelling will be presented and some special challenges arising from NPs will be emphasized. For carbon nanodots studies revealing their surprisingly narrow sub 1 nm size were conducted[3]. The effect of photobleaching was further studied by means of AUC[4].
Studies on CuInS2 NPs were carried out to determine their sedimentation coefficient distribution. The acquisition of MWL data during the sedimentation process allowed for the analysis of size dependent optical properties at the same time.
A third project focuses on the multidimensional analysis of polydisperse particle size distributions (PSDs). Current direct boundary tools either show a lack in resolution or are not suited for the analysis of broad PSDs. We developed a new methodology for the simultaneous determination of size and density for polydisperse PSDs based on the parametrically constrained spectrum analysis implemented in Ultrascan3. It allows us to derive core-shell properties of NPs while preserving high resolution for the sedimentation coefficient.
We believe that MWL-AUC in combination with high-performance data evaluation is a powerful technique as the direct correlation of size, shape and optical properties of NPs is highly relevant for a variety of new applications where multidimensional particle properties are in the focus.

[1] W. Cao and B. Demeler, Biophys. J., 2005, 89, 1589.
[2] E. Brookes, W. Cao and B. Demeler, Eur. Biophys. J., 2010, 39, 405.
[3] V. Strauss, J. T. Margraf, C. Dolle, et al., J. Am. Chem. Soc., 2014, 136, 17308.
[4] W. Wang, C. Damm, J. Walter, et al., Phys. Chem. Chem. Phys., 2016, 18, 466.

Fluid Mechanics

[ST 1] Fire Simulation in Underground Stations

B. Schröder, A. Meunders, ***L. Arnold***

Underground train stations are complex facilities with challenging structural features for preventive and defensive fire protection. Additionally these facilities are frequented by large numbers of passengers that primarily depend on self-rescue in case of a fire. Over the course of an incident the design of the stations also has to support effective rescue and extinguishing measures by the fire brigades. To satisfy overall safety objectives the compliance of predefined performance criteria has to be proven. Increasingly numerical methods are being used for this purpose.
Multiple studies have demonstrated the use of CFD-models to perform fire scenario analysis in underground stations. Usually the simulations concern one existing station with one predefined design fire and consider only a few parameters e.g. the location of the seat of fire or the position and dimension of ventilation components. However there are many other parameters that effect the prediction of the spread of smoke and hot gases (i.e. a heterogeneous design fires, weather-induced airflows or characteristic structural features). The resulting effects stem from a combination of multiple and non-linear parameters which in general, do not refer to a single distinguished set of parameters, but a probability distribution.
Regarding structural features we refrain from individual case studies to achieve more generic conclusions. Several stations in Germany have been examined and reduced to a set of standard types. A wide set of design fires is considered. In this way it is possible to cover different fire safety performance levels of rolling stock as well as the results of various full- and mid-scale tests.
A special focus of this work is the persistent air movement in metro stations. Underground tunnel networks, including stations, provide very special climatic conditions. The airflows are not only induced by train traffic, but also by temperature gradients and ambient weather conditions. These traffic-independent flows can drastically influence the propagation of smoke and hot gases as well as the natural ventilation itself. Based on longterm measurements and climate modelling, we apply flow boundary conditions to our generalised station design. For the outlined work we utilize mathematical techniques, such as screening and orthogonal sampling, to overcome the high dimensional parameter spaces. The response parameters (e.g. smoke layer heights, temperature distributions etc.) are calculated with FDS. The high computational demands of the considered investigations necessitate the use of high performance computing facilities. Due to the extent of the sampling process, automation is inevitable. This includes the preparation of FDS-input files, batch-based multiple job execution and post-processing.

[ST 2] Blood Flow Analysis in the FDA Centrifugal Blood Pump

M. Behbahani*, V. Marinova, A. Lintermann, C. Moulinec, J. H. Göbbert, I. Kerroumi, Y. Fournier, S. Rible*

Ventricular Assist Devices (VADs) are commonly implanted to assist patients suffering from heart disease. They provide long- and short-term support for the human heart and help patients to recover from heart attacks and from congestive heart failure. It is essential to design bloodsensitive VADs to minimize the risk of hemolysis and thrombosis. The blood pump, however, must operate at a wide range of flow rates and pressure heads which makes a low-risk design a challenging task. In this study the flow in a centrifugal blood pump, provided by the U.S. Food and Drug Administration (FDA), is investigated by means of numerical simulations on high performance computers. The simulations are carried out for

different operation Reynolds numbers. A total of 15 pump revolutions is performed to obtain quasi-steady results. The pressure drop across the pump is considered to study convergence of the solution and to characterize the energy loss of the device. Investigations of the velocity field show that there exist high velocities and strong velocity gradients and shear layers in the outflow region potentially leading to hemolysis. Different turbulence models including RANS and LES are tested. Finally, the motor torque is investigated to identify the force acting on the blades. All the findings show that there is a strong need to develop more blood-sensitive designs to reduce the risk of hemolysis and thrombosis.

[ST 3] High-Fidelity Multiphase Simulations and *In Situ* Visualization Using CIAO

***M. Bode**, J. H. Göbbert, H. Pitsch*

The performance of current fuel injection systems depends on a cascade of physical processes originating from the nozzle internal flow, possible occurrence of cavitation, turbulence, and the mixing of a coherent liquid stream with a gaseous ambient environment. The interaction of these processes is not completely understood yet and the design of injectors leading to efficient mixing, combustion, and subsequent reduction of pollutant formation and emissions is still a big challenge.
Typical diesel injection systems, for example, inject the fuel at about 600 m/s and have outlet diameters of the order of 100 micrometers, which is the size of a hair. The size of the resulting smallest droplets and turbulent structures is even much smaller. This illustrates two of the major problems for designing current injectors: First, experiments characterizing the atomization process are very difficult due to the small length scales. Second, huge meshes are required for simulating injection processes, because of the necessity to resolve the broad spectrum of length scales in play within a single simulation. Therefore, it is not possible to study complex injection systems without using massively parallel code frameworks and supercomputers.
A new simulation framework, which enables highly accurate and predictive simulations of fuel injection processes was established for this work as part of the CIAO code and relies on three recent developments: First, new numerical methods for large-eddy simulations (LES) of compressible nozzle flows including an equation-of-state based cavitation model were adapted. Second, new methods for simulating the primary breakup in the vicinity of the nozzle exit were investigated. These are based on a 3D unsplit forward/backward Volume-of-Fluid (VOF) approach that is coupled to a Level Set (LS) method (3DU-CLSVOF) and a hybrid discretization of the convective transport term and of the pressure-projection. Third, the framework was extended to couple the highly accurate results of the primary breakup simulations to Lagrangian-particle-based spray simulations in order to achieve results for the spray evolution further downstream of the nozzle with currently available computing resources.
In this project, the performance of the CIAO code was improved in order to show good scalability on all cores of JUQUEEN and become a member of JUQUEEN's High-Q Club. Furthermore, the use of the *in situ* visualization library VisIt was established on JUQUEEN in order to significantly reduce the resulting amount of simulation data during runtime without losing relevant simulation results. Finally, the new code framework was applied to current diesel and gasoline injectors and fundamental mechanisms of fuel injection are studied. One example is the impact of cavitation on the liquid cone angle and the resulting spray characteristics. This correlation is crucial for improving spray models currently used in industry.

[ST 4] Instabilities and Turbulence in Magnetohydrodynamic Duct Flow

D. Krasnov, V. Bandaru, ***T. Boeck***

We study flows in rectangular ducts in the presence of a uniform magnetic field, which are prototypical configurations of liquid-metal flows in metallurgical applications and cooling blankets of nuclear fusion reactors. Numerical simulations are an important research tool in this field because the liquid metals are typically hot and agressive, which poses a significant problem for traditional measurement methods where a sensor is in contact with the fluid. Since the metals are non-transparent optical measurement methods cannot be used either.
In the fusion blankets lead-lithium circulates through a system of ducts in order to breed tritium and to extract heat. The ducts are typically made from metals, i.e. the walls are conducting. Under the influence of a magnetic field a strong braking force occurs in the core of the duct. Near the walls parallel to the magnetic field the Lorentz force is weak, which leads to the formation of strong jets at these walls. These jets are prone to shear instabilities, which give rise to turbulence. We study these side-layer instabilities and the transition to turbulence through numerical simulations. The resolution requirements are high because the side layers become very thin in strong magnetic fields. We find localized patches of turbulence with specific vortical structures as well as continuous turbulent bands at higher Reynolds numbers.
We also study flows with insulating walls at finite magnetic Reynolds numbers, i.e. with independent dynamics of the magnetic field. In this case the magnetic field has to be solved in the interior of the duct as well as in the exterior, and its continuity has to be ensured on the duct walls. To account for the exterior field one can formulate non-local boundary conditions for the magnetic field on the duct walls by a boundary-element method. We have implemented this approach in a numerical code and perform simulations of duct turbulence at finite values of the magnetic Reynolds number. Compared with the case of negligible magnetic Reynolds number the turbulence near the Hartmann walls perpendicular to the magnetic field is enhanced.

[ST 5] Stochastic Aspects on 3D Simulation of Transport Processes in Fibrous Microstructures, Using the Lattice Boltzmann Method

D. Froning*, J. Yu, U. Reimer, V. Schmidt, W. Lehnert*

The gas diffusion layer (GDL) is a key component of fuel cells based on polymer electrolyte membranes (PEFC, DMFC and HT-PEFC). The efficient operation of fuel cells requires good transportation properties of GDL which allow educts to reach the electrodes out of the gas channels as well as to transport products from the electrodes back to gas channels.
The microstructure of GDL is taken from a stochastic model which creates 3D structures from 2D SEM images. The details of the stochastic methods, their application and the model validation via full 3D information of the microstructure from images gained by synchrotron X-ray tomography has been developed at the Ulm University [1].
In this way, the numerical simulations are based on a geometry which is of stochastic nature. As a conclusion, all results from numerical simulations on such geometries are expected to show stochastic behavior even if they are calculated numerically. We show that an ensemble of geometries – all of them realizations of the stochastic simulation model – leads to results that can be interpreted under a stochastic view. We take special account on the tortuosity of sections of different sizes of a GDL to show the potential of a combined stochastic and numerical modeling for fuel cell research.
The general objective of our research is the construction of microstructures of GDL which are favorable for mass transport in fuel cells. Preliminary investigations of GDL microstructures with respect to transport relevant structural properties have been reported in [2]. In the present work, we go one step further and investigate transport properties of GDL not only by considering structural characteristics, but incorporating numerical models for transport

processes. Therefore simulations of transport processes by means of the Lattice Boltzmann method are applied, where the stochastic model for the microstructure mentioned above is used in order to generate the underlying geometric structures [3].
This research was funded by the German “Federal Ministry of Education and Research“, grant 03MS507C. Simulations are running on hardware of the Jülich Supercomputing Centre, grant JIEK30.

[1] R. Thiedmann, F. Fleischer, C. Hartnig, W. Lehnert, V. Schmidt. Stochastic 3D modelling of the GDL structure in PEM fuel cells, based on thin section detection. Journal of the Electrochemical Society 155 (2008) B391-B399.
[2] R. Thiedmann, C. Hartnig, I. Manke, V. Schmidt, W. Lehnert (2009) Local structural characteristics of pore space in GDL’s of PEM fuel cells based on geometric 3D graphs. Journal of the Electrochemical Society 156 (2009) B1339-B1347.
[3] D. Froning, J. Brinkmann, U. Reimer, V. Schmidt, W. Lehnert, D. Stolten. 3D analysis, modeling and simulation of transport processes in compressed fibrous microstructures, using the Lattice Boltzmann method. Electrochimica Acta 110 (2013) 325-334.

[ST 6] The Local Structure of Turbulent Flows at High Reynolds Numbers

***M. Gauding**, J. H. Goebbert, F. Dietzsch, C. Hasse*

Small scale turbulence continues to be one of the unsolved problems of classical physics. The turbulent motion of fluids is a highly complex phenomenon and its statistical description and modeling is challenging. Conventional concepts, in the spirit of Kolmogorov's scaling theory, were only partially successful and failed in explaining phenomena like intermittency and anomalous scaling. A new view on turbulence has been given by the method of dissipation elements. The method of dissipation elements provides a decomposition of the turbulent field in space-filling sub-units, which are statistically parameterized by two quantities, a length scale and a scalar difference. This decomposition reduces the complexity of the problem, but retains information about the local structure of turbulent fields, which would be lost otherwise when taking an ensemble-average. Knowing the decomposition of the turbulent field in terms of dissipation elements, one is able to compute conditional statistics, or alternatively, to detect coherent structures that are coupled through a diffusive layer. As a consequence, our approach can isolate specific local phenomena that are not accessible by conventional statistics.
We present a variety of different highly resolved direct numerical simulations (homogeneous isotropic turbulence, turbulent jet flow, turbulent non-premixed flame) that have been performed on the supercomputer JUQUEEN. The biggest run has more than 68 billion grid points. The data base has been analyzed by conventional statistics and by the method of dissipation elements. An emphasis of the analysis is put on internal and external intermittency.

[ST 7] Passive and Active Scalar Mixing in Turbulence

***P. Götzfried**, M. S. Emran, R. A. Shaw, B. Kumar, J. Schumacher*

Three-dimensional direct numerical simulations of a shearless mixing layer are performed with a hybrid Euler-Lagrange model in order to study the mixing and subsequent entrainment of active scalar fields. These studies are conducted in order to understand the coupling of small-scale turbulence with cloud water droplets at the edge of a turbulent cloud. Furthermore we perform Lagrangian tracer simulations in order to investigate the mixing of passive scalars in a simple turbulent flow at high Schmidt numbers.

[ST 8] Turbulent Convection at Very Low Prandtl Numbers

J. D. Scheel, A. Kolchinskaya, ***J. Schumacher***

We investigate turbulent convection in liquid metals at large Rayleigh numbers by means of highly resolved direct numerical simulations. These convection flows are characterized by very small Prandtl numbers. Although this class of turbulent flows obeys many important applications reaching from solar convection via liquid metal batteries to nuclear engineering, laboratory experiments are rare. Supercomputer simulations can fill this gap and reveal the structure formation and the related mechanisms of turbulent heat transfer.

[ST 9] Parallel Stabilized Finite Element Methods for Aero-, Hemo- and Hydrodynamics

M. Brüderlin, M. Danwitz, M. Frings, S. Haßler, J. Helmig, N. Hosters, V. Karyofylli, P. Knechtges, M. Make, A.E. Öngüt, L. Pauli, R. Siegbert, A. Stavrev, L. Wendling, F. Zwicke, S. Elgeti, M. Behr

The objective of this project is the (continued) development of effective simulation methods for unsteady flows of fluids, including microstructured liquids, in situations involving significant deformations of the computational domain. These methods are based on the finite element technique, using stabilized formulations, unstructured three-dimensional meshes, and iterative solution strategies. The parallel implementation is based on the message-passing communication libraries, and is portable across a wide range of computer architectures.
The main areas where novel computational methods are being developed are:

- simulation of flows in the presence of rapidly translating or rotating boundaries, using the Shear-Slip Mesh Update Method (SSMUM),
- simulation of flows of microstructured liquids including the effect of flow on the microstructure in case of blood,
- simulation of non-Newtonian fluids,
- simulation of two-phase and free-surface flows, and
- shape optimization of complex geometries with applications in shear-thinning fluids and free-surface filling processes.

These simulations are done in the scope of different subprojects. The non-Newtonian fluid models are used in the simulation of centrifugal and axial pump hemodynamics. They also describe the behaviour of molten plastic in the shape optimization of complex plastics profile extrusion dies. Moving and rotating boundaries are part of nearly all applications.

Earth and Environment

[MET 1] Benefits of an Ultra Large and Multiresolution Ensemble for Estimating Available Wind and Solar Power

***J. Berndt**, C. Hoppe, H. Elbern*

In this study, we present a highly parallel efficient and comprehensive ensemble setup of an atmospheric model within a particle filtering environment.
In an increasing number of atmospheric modeling tasks, the need for probabilistic forecasts is becoming more and more urgent. This is especially true for probabilistic forecasts for renewable energy prediction, specifically energy meteorological forecasts. Notably, (i) stable power grid management and (ii) information for the electricity market, realized by power stock exchange, need predictions for the ”intra-day” trade in 15-minute resolution. These predictions must be furbished with likelihood, leading to a probabilistic approach. The only feasible, yet novel approach is a transition to stochastic extensions of the meteorological models, leading to the integration of ensemble models.
In the short and medium prediction range, current wind and solar power forecast systems meanwhile rest on NWP ensemble models and show satisfying average forecast accuracy. However, only calibrated ensembles from meteorological institutions serve as input so far, with limited spatial resolution (∼10 − 80 km) and low member number (∼ 50). Perturbations related to the specific merits of wind and solar power production are still missing.
We therefore investigate the benefits of a short-term (1 to 48 hour) scaled and balanced high-resolution (≈ 1 km) meteorological ensemble using an ultra large ensemble size with up to O(1000) members. The numerical forecast model used in this project is the Weather Research and Forecasting Model (WRF). We use different ensemble systems from global models (ECMWF and GFS) as input and boundary to capture different synoptic conditions. Model uncertainties are represented by stochastic parametrization of sub-grid processes via stochastically perturbed parametrization tendencies and in conjunction via the complementary stochastic kinetic-energy backscatter scheme. We perform continuous ensemble updates by comparing each ensemble member with available observations using a sequential importance resampling filter as a nonlinear data assimilation technique. This requires a dynamical update with inter-member communication during runtime and therefore a second stage of parallelism has been introduced into WRF, which allows to perform an ensemble run by one executable guaranteeing computational efficiency. In this context, code adaptation has been carried out to fit the JUQUEEN's architecture. Corresponding performance plots are presented.

[MET 2] Computational Aspects of High-Resolution Global Gravity Field Determination

***J. M. Brockmann,** W.-D. Schuh*

Estimating a model of the Earth's gravity field from complementary observation types is a computationally demanding task. Global gravity field models are typically described as a spherical harmonic series up to a certain maximal degree which corresponds to the spatial resolution of the model. The computational effort depends on the one hand on the maximal resolution of the spherical harmonic expansion (i.e. the number of parameters to be estimated, e.g. tens to hundreds of thousands) and on the other hand on the number and the stochastic properties of the observations (e.g. up to hundreds of million highly correlated observations). If computationally motivated approximations (e.g. block-diagonal approximations) should be avoided, concepts of high-performance computing have to be used to compute rigorous least-squares solutions from a typically dense highly overdetermined system of equations.

Within this contribution we will provide an overview of the computational aspects of global gravity field determination based on observations collected by satellites. Whereas the spatial resolution of so called "satellite-only" models is limited (75 - 100 km, less than 60 000 - 90 000 unknown parameters) a huge number of typically highly correlated measurements is collected by the dedicated satellites. Due to the correlations, advanced decorrelation strategies are required to derive the optimal solution in a least squares sense. In addition to the solution, the accuracy description in terms of a full covariance matrix becomes more and more important for the further use of the gravity field model in advanced applications from oceanography or geophysics. Based on the satellite mission GOCE the poster will present an overview of the computational challenges. Including altimetric sea surface height measurements the dynamic ocean topography can be estimated in addition to the Earth's gravity field. Based on a local estimation of the mean dynamic topography in the North Atlantic, the computational challenges are summarized for different finite element based parameterizations of the the ocean's dynamic topography. Future current studies and challenges are discussed in an outlook.

[MET 3] Water Flow and Permeability Distribution in a Tectonically Limited Hard-Rock Aquifer

***J. Bruckmann**, D. Burs, C. Clauser, T. R. Rüde*

Groundwater systems are often characterized by heterogeneous aquifer systems due to spatial variability of hydraulic properties. Especially in hard-rocks with a complex tectonic history hydraulic properties tend to be strongly spatially variable. At the same time only a limited amount of direct measurements or indirect data characterizing subsurface flow is available from boreholes. Yet, assigning adequate hydraulic properties to hydrological units is crucial for a proper groundwater flow assessment. One possibility for addressing subsurface parameter heterogeneity and uncertainty in numerical models are stochastic inversion methods. Among them is the Monte Carlo (MC) approach which is based on statistical analysis of a large number of randomly created, equally likely forward simulations. Generation of such an ensemble of model realizations is based on given probability distributions of model parameters as well as information on the parameter’s spatial correlation.
Here, we study the active drinking water production site Hastenrather Graben near Eschweiler, Germany. A three dimensional structural subsurface model of the structurally complex and heterogeneous aquifer system provides the basis for numerical simulations. A subset of around 3.6 km in E-W direction, 2.9 km in N-S direction and 720 m depth is divided into a rectilinear grid with a uniform cell size of 10 m x 10 m x 10 m, resulting in nearly 7.5 Million grid cells. This discretization is necessary for resolving the folded hard-rock aquifer and its structural limitations sufficiently. Numerical simulation of groundwater flow in such a large model is only feasible using high-performance computing. We use the parallel code package SHEMAT-Suite for numerical simulations of groundwater flow with the finite difference method and for stochastic inversion for analyzing the permeability distribution of the hard-rock aquifer. We present the subsurface model of the study area and the resulting setup of the numerical model. Additionally, we show first results of permeability estimation using stochastic inversion. Simulations are performed on the JARA-HPC partition part of the supercomputer JURECA at Jülich Supercomputing Centre.

[MET 4] High Dimensional Application of Combined Four Dimensional Variational Data Assimilation and Particle Filtering for Estimating Volcanic Ash Emissions

***P. Franke**, A. C. Lange, H. Elbern*

Presented is an ensemble based optimization of high temporal resolved volcanic emission profiles using a new developed Sequential Importance Resampling Smoother. To estimate volcanic ash emissions and its uncertainty using a chemistry transport model and its adjoint requires an ensemble of model runs. This has recently become feasible due to supercomputers provide the necessary computational resources.
Estimating volcanic ash emissions adequately is a very challenging task due to limited monitoring techniques of the ash plume and nonlinear processes in the atmosphere, which make application of remotely sensed data difficult. Most models which estimate volcanic ash emissions use inappropriately simplified atmospheric processes underlying the dispersion of volcanic ash.
The objective of this work is to provide volcanic ash emissions using a full chemistry transport model and its adjoint as well as an ensemble of model runs to quantify forecast uncertainties. Therefore, the four dimensional variational data assimilation version of the EURAD-IM chemistry transport model is extended to a Sequential Importance Resampling Smoother using new weighting and resampling strategies. In the main step the ensemble members exchange high valued emission patterns while rejecting emission patterns with low value for the forecast. The emission profiles of the ensemble members are perturbed to guarantee different emissions for all ensemble members.
First identical twin experiments show the ability of the system to estimate the temporal and vertical distribution of volcanic ash emissions. The 4D-Var data assimilation algorithm of the new system additionally provides quantitative emission estimation.

[MET 5] Model Development for Meteorological Application

*M. Baumann, S. Gawlok, M. Wlotzka, **P. Gerstner**, T. Beck, V. Heuveline*

The dynamical behavior of the atmosphere is related to processes on a wide range of spatial and temporal scales that must be accounted for during numerical modeling. The task of predicting the evolution of tropical cyclones (TCs) is a typical challenging example. A storm's behavior is mainly determined by large-scale flows in the order of several thousand kilometers whereas processes on much smaller scales, down to less than km, are important for the intensity evolution. Typically, not all of the relevant scales can be resolved in numerical simulations due to restrictions of available computer resource and an adequate choice of the physical model equation as well as a suitable discretization and solution method are essential for efficient modelling of the atmosphere.
We investigated that part of a model system which describes the fluid dynamics and the effects of buoyancy due to temperature differences. We considered a hierarchy of physical models consisting of the incompressible Navier-Stokes equations with a Boussinesq forcing, a Low-Mach model, and the full compressible Navier-Stokes equations.
In general, benchmarking of numerical models requires some evaluation ability of the quality of some model's output. In contrast to many other disciplines, for most meteorological applications benchmarking is complicated since a fixed state of the atmosphere cannot be reproduced again. Therefore, it is well-motivated to investigate laboratory experiments which are relevant for atmospheric considerations as benchmark problems to evaluate numerical models. In case of experiments, the quality evaluation of model outputs can be done based on measurements and no *a priori* assumption about the "best model", which should serve as reference solution, is needed.
Such scenarios are very valuable in cases where assumptions and simplification on the level of the model equation, e.g. Boussinesq approximation, are questionable and should be

investigated. We continued our investigation of the baroclinic wavetank laboratory experiment and the scenario of two interacting tropical cyclones started in the first phase of our project HKA14.

[MET 6] A Novel Coupled Physical-Biogeochemical Model System for the Southern North Sea

***R. Hofmeister**, C. Lemmen, K. Wirtz, O. Kerimoglu*

Here we present a novel adaptive biogeochemical model, applied in a decadal hindcast simulation of the southern North Sea, where it is coupled to a 2-D benthic model and a 3-D hydrodynamic model in an approximately 1.5 km horizontal resolution at the German Bight coast. The model is shown to have good skill in terms of resolving the salinity, temperature, dissolved nutrient and chlorophyll gradients in the German Bight. We perform a scenario analysis to gain insight into the effects of the aimed nutrient reduction loads in the major German and Dutch rivers on the system.
The modular model system also enables to couple a 3-D sediment diagenesis model instead of the 2-D benthic model, such that pore-water nutrient profiles, denitrification, and oxygen penetration into the sediment can be resolved.

[MET 7] Very High Resolution Simulations of African Climate with the Regional Climate Model REMO

A. Hänsler, N. Koldunov, D. Sein, W. Sauf, ***D. Jacob***

The regional climate model REMO is used to perform high resolution simulations of African climate. Simulated seasonal precipitation is analyzed and compared to a lower resolution run and observational data. We show that the high resolution model is able to represent small scale features of the precipitation distribution and therefore demonstrates considerable improvement compared to lower resolution version. We also assessed the performance of REMO on the JUQUEEN supercomputer (Jülich Supercomputing Centre, JSC) and found, that it is not the optimal system for conducting regional climate model simulations. Computers with architecture similar to JUROPA or JURECA (JSC) are better suited for this type of applications.

[MET 8] First-Principles Prediction of Ni Partitioning between Silicate and Metal Melts

D. Künzel, J. Wagner, ***S. Jahn***

Most geological processes are accompanied by a re-distribution of elements between different phases. Element partition coefficients between minerals, melts and fluids have been measured for many systems. The lattice strain model of Blundy and Wood (1994) has been very successful to explain mineral-melt partitioning of trace elements in terms of crystal chemistry. However, a more general theoretical framework for element partitioning is still missing. Here, we explore a first-principles simulation approach to predict element partition coefficients between metal melts and silicate melts, which may be considered a model system for metal-silicate segregation during the early evolution of the Earth, which eventually lead to core formation. The simulations provide simultaneous access to the atomic structure and to thermodynamic state variables. Using the alchemical transmutation method of thermodynamic integration, the equilibrium constants of exchange reactions, e.g., of Ni and Fe between metal and silicate melts are estimated. Structurally, Ni and Fe have a very similar coordination environment in the metal melt, whereas Ni-O bonds in silicate melts are considerably longer

than Fe-O bonds. The derived Ni partition coefficients agree rather well with experimental data, which provides confidence in the computational method used here. Relations between melt structure and partitioning behavior and the potential of predicting other partition coefficients from first-principles will be discussed.

Blundy and Wood (1994) Nature 372, 452-454.

[MET 9] Validation of the SACADA 4D-Var Assimilation System with the High Resolution Retrievals from CRISTA-NF and MLS

***K. Kasradze**, H. Elbern, J. Schwinger*

SACADA (Synoptic Analysis of Chemical constituents by Advanced Data Assimilation) is a four-dimensional variational assimilation system developed for estimation of transport and chemical transformation of atmospheric trace gases in stratosphere. A novel global chemistry transport model with its adjoint version is the kernel of this system. The German Weather Service global forecast model (GME) is used as an online meteorological driver, also with its icosahedral grid structure and the horizontal transport algorithm. Recently, the horizontal and vertical scheme resolution of the model grid was refined: The resolution of the horizontal grid points was increased to about 150 km and vertical separation between grid levels is now less then 1 km below 22 km altitude. The parallel performance has been evaluated. The chemistry module of the SACADA was extended and revised to better represent chemical processes in the lower stratosphere/upper troposphere (UT/LS). All this modifications were done in order to draw full advantage from high resolution limb sounding instruments, like CRISTA-NF (Cryogenic Infrared Spectrometers and Telescopes for the Atmosphere - New Frontiers) of IEK-7 (Institute of Energy and Climate Research - Stratosphere, Research Centre Jülich). As a case study, assimilation of MLS data with diagnosis of observation and background error statistics in observation space for H2O was performed. Relative humidity is used to filter observations and the background field. It is shown that the H2O analysis significantly improves compared to the ECMWF operational analysis. Additionally, data from the CRISTA-NF instrument, which has been operated on board the Russian high altitude research aircraft M-55 Geophysica, was assimilated. These CRISTA-NF observations have been taken during the SCOUT-AMMA Campaign in summer 2006 by IEK-7. A basic finding is that the H2O-analysis based on the additional CRISTA-NF data in the UT/LS region improves with the SACADA high resolution configuration.

[MET 10] The Centre of High-Performance Scientific Computing, Geoverbund, ABC/J – Geosciences Enabled by HPSC

***S. Kollet**, K. Görgen, H. Vereecken, F. Gasper, H.-J. Hendricks-Franssen, J. Keune, K. Kulkarni, W. Kurtz, W. Sharples, P. Shrestha, C. Simmer, M. Sulis, J. Vanderborght*

The Centre of High-Performance Scientific Computing (HPSC TerrSys) was founded 2011 to establish a centre of competence in high-performance scientific computing in terrestrial systems and the geosciences enabling fundamental and applied geoscientific research in the Geoverbund ABC/J (geoscientfic research alliance of the Universities of Aachen, Cologne, Bonn and the Research Centre Jülich, Germany). The specific goals of HPSC TerrSys are to achieve relevance at the national and international level in (i) the development and application of HPSC technologies in the geoscientific community; (ii) student education; (iii) HPSC services and support also to the wider geoscientific community; and in (iv) the industry and public sectors via e.g., useful applications and data products. A key feature of HPSC TerrSys is the Simulation Laboratory Terrestrial Systems, which is located at the Jülich Supercomputing Centre (JSC) and provides extensive capabilities with respect to porting,

profiling, tuning and performance monitoring of geoscientific software in JSC's supercomputing environment. We will present a summary of success stories of HPSC applications including integrated terrestrial model development, parallel profiling and its application from watersheds to the continent; massively parallel data assimilation using physics-based models and ensemble methods; quasi-operational terrestrial water and energy monitoring; and convection permitting climate simulations over Europe. The success stories stress the need for a formalized education of students in the application of HPSC technologies in future.

[MET 11] The Data Assimilation Framework TerrSysMP-PDAF: Data Assimilation for Integrated Terrestrial System Models

***W. Kurtz**, G. He, S. Kollet, R. Maxwell, H. Vereecken, H.-J. Hendricks Franssen*

Modeling of terrestrial systems is continuously moving towards more integrated modeling approaches where different terrestrial compartment models are combined in order to realize a more sophisticated physical description of water, energy and carbon fluxes across compartment boundaries and to provide a more integrated view on terrestrial processes. An example of such an integrated earth system model is the recently established modeling platform TerrSysMP consisting of individual component models for variably saturated subsurface flow (ParFlow), land surface processes (CLM 3.5) and weather forecast (COSMO-DE). The component models are dynamically linked by the exchange of state variables and fluxes with the coupling software OASIS-MCT in a modular, scale-consistent manner which provides a fully coupled representation of terrestrial processes. Nevertheless, predictions with TerrSysMP are affected by uncertainty given the many unknown input parameters. Data assimilation can potentially improve the model predictions and reduce the uncertainty by updating model simulations with real-time measurement data. Measurement data also allow improving the characterization of the model parameters and thus long-term climate simulations. Therefore, we developed a data assimilation system in combination with TerrSysMP by coupling TerrSysMP with the PDAF (Parallel Data Assimilation Framework) library. PDAF is specifically designed for parallel simulation models and provides a variety of global and local data assimilation algorithms. The data assimilation framework TerrSysMP-PDAF uses a memory based communication between model and data assimilation routines and avoids frequent re-initializations of the model and is thus highly scalable and applicable to large scale hydrological systems. This presentation provides an overview on the TerrSysMP-PDAF data assimilation system including results for the assimilation of data from cosmic ray probes to improve the catchment-wide characterization of hydrological fluxes.

[MET 12] Seismic Applications of Elastic and Acoustic Full Waveform Inversion to Field Data

*M. Binnig, M. Kunert, **A. Kurzmann**, L. Gaßner, N. Thiel, T. Bohlen*

An important objective of seismic surveys in geophysics is to characterise the structure of Earth's subsurface. In contrast to conventional (ray-based) imaging methods, full waveform inversion (FWI) exploits the full content of seismic data in order to reconstruct high-resolution parameter models at sub-wavelength scales. Furthermore, it helps to improve petrophysical interpretation by assigning physical parameters, such as seismic velocities, to structural images obtained by classical methods.
In this work, we present two field-data applications, representing the capabilities of FWI. In the first example we applied elastic FWI to surface waves. Those Rayleigh waves have a high sensitivity to the shear-wave velocity and, thus, are attractive to derive geotechnical parameters of the very shallow subsurface. Based on the application of 2D FWI to Rayleigh

waves, we reconstructed the shape of a refilled trench (part of a former defensive wall during the "War of the Spanish Succession", the so-called "Ettlinger Linie") by identifying a zone of reduced shear-wave velocity. The second example shows the application of acoustic FWI to marine seismic data obtained in a river delta with potential oil and gas deposits. We recovered two types of low-velocity zones from compressional waves: small-scale anomalies in layered sediments and extended structures. The results of a conventional and different seismic imaging method substantiates our interpretation: existence of potential gas accumulations in shallow areas close to the seafloor and deeper geological faults.

[MET 13] New Insights into Boundary-Layer Turbulence Gained from Direct Numerical Simulations

***J. P. Mellado**, C. Ansorge, A. de Lozar, C. van Heerwaarden, T. Keitzl*

The Planetary Boundary Layer (PBL), the part of the atmosphere that is in contact with the surface and that feels the cycle of day and night, regulates the exchange of mass, momentum and energy between the rest of the atmosphere and the land and the oceans. This exchange strongly depends on how turbulence interact with other phenomena, such as density stratification, interfaces, radiation, or clouds. Still, the current understanding of this interaction remains incomplete, which translates into important uncertainties in atmospheric models. By providing a faithful description of turbulence across all relevant scales, without any turbulence model, Direct Numerical Simulation (DNS) is opening new avenues to advance this understanding. This poster illustrates this novel approach, presenting studies of stably stratified and unstably stratified PBLs, as well as studies of entrainment at the top of stratocumulus clouds.

Most atmospheric models rely on flux parametrizations providing the lower boundary conditions and vertical diffusivities in the vicinity of the lower boundary, and the correct prescription of those properties remains a challenge. To study the stable PBL, we use Ekman flow with an appropriate Dirichlet boundary condition. We can reproduce weakly, intermediately and strongly stratified turbulence, including global intermittency, by varying one single parameter (a bulk Richardson number). By means of conditional analysis, we have shown that much of the effect of global intermittency on conventional statistics is caused by changes in the intermittency factor, whereas the turbulence inside the turbulence pockets remains approximately similar. Regarding the unstable PBL, we have parameterized transitions between the macro-, meso- and micro-scale regimes as a function of surface heterogeneity. For the first time, one single simulation has covered all three regimes. In contrast to previous understanding, we have shown that transitions do not occur at a fix ratio of PBL height to heterogeneity size, but earlier for larger heterogeneity.

Regarding stratocumulus-top entrainment, understanding the interaction between turbulent mixing and cloud-top cooling has remained a challenge during decades: it is difficult to study such small-scale processes, of the order of tens of meters or less, but they are important on a planetary scale because of the their effect on the earth's radiative balance. During the last year, we have quantified the relevance of cloud-droplet evaporation. First, we have shown that wind shear at the cloud-top can act as a catalyst of evaporative cooling and lead to entrainment rates in agreement with measurements. Second, we have shown that the contributions from evaporative and radiative cooling to entrainment rates are comparable to each other, and we have developed parametrizations that represent this relative contribution.

[MET 14] Forward and Inverse Modeling of Lithospheric Deformation on Geological Timescales

B. J. P. Kaus, ***A. A. Popov,*** *G. Reuber, T. S. Baumann, A. E. Püsök, A. Bauville, N. Fernandez, M. Collignon*

Geological processes such as mountain belt formation, subduction of tectonic plates and the development of sedimentary basins occur on a million-year timescale and involve rocks that have nonlinear visco-elasto-plastic material properties and experienced very large deformations. In order to simulate such processes in 3D, we developed a scalable parallel code, LaMEM, that employs a staggered finite difference discretization combined with a marker and cell approach. Here, we describe the numerical approach and discuss some case studies in which we employed the code (i) to study the physics of crustal scale folding and faulting, (ii) to understand how continental collision might result in mountain belt and plateau formation, (iii) how it can be combined with an inversion strategy to constrain the rheology of the crust and lithosphere.

[MET 15] Ocean Turbulence Control of Climate

M. B. Poulsen*, C. Eden, M. Jochum*

The Atlantic Meridional Overturning Circulation (AMOC) transports warm tropical surface water toward northern Europe and returns cold water at depth to the world's ocean. At the same time it plays a significant role in the global carbon cycle through the ocean's ability to dissolve carbon dioxide. This overturning is thus of great climatic importance, but a complete picture of its driving forces has not yet emerged due to several observational and theoretical challenges.
One of the leading hypotheses on what governs the AMOC strength is the strong westerly winds that overlie the Southern Ocean (SO). In combination with the unique basin geometry, these winds are able to supply the necessary energy to raise the water from great depths to the surface and return it back towards equator. This idea has gained support from past numerical model studies, but which did not include the explicit effect of ocean mesoscale eddies.
Recent research has shown that instability of the Antarctic Circumpolar Current (ACC) in the SO fuels a rich eddy field, which compensates the effect of the winds on the overturning in the SO. These studies have however been idealized with respect to bottom topography, basin geometry and governing equations, all of which are aspects of the SO that is known to be important to the dynamics. Present day state-of-the-art climate models, like the Community Earth System Model (CESM), relax these simplifications by solving the full set of equations in a more realistic domain, but are too crude in resolution to explicitly resolve ocean eddies, why they need be parameterized. This involves a complication due to the necessary specification of an eddy diffusivity.
Since the middle of the last century the SO winds are observed to have increased by up to 30% in strength. Given the potential impact on the AMOC and hence the climate, it is crucial to determine the correct ocean response to wind changes. A wind stress perturbation experiment using CESM with resolved ocean mesoscale eddies (1/10 of a degree in horizontal resolution, about 108 grid points) is therefore conducted on Juqueen using 4096 cores.
The model is forced with climatology through the first 25 model years, after which the wind stress in the SO is increased by 50% and the model is run for another 20 years. The model outputs every third model day, generates 12TB of data each model year, and output is transferred to the Niels Bohr Institute on a daily basis. Presently eight model years of integration has been completed since the onset of the perturbation, and the model ocean has not yet reached a new equilibrium. Depending on the new steady state of the ACC and the

AMOC, it will be possible to either reject or confirm the hypothesis that the SO winds are the key control of the AMOC strength.

[MET 16] High Optimization of Initial Values and Emission Factors by 4D-Var Data Assimilation Encoded on a Mesoscale Air Quality Numerical Modelling System

***I. Ribeiro**, Z. Paschalidi, H. Elbern*

Advanced space-time data assimilation and inverse modelling algorithms, combining observations with numerical models require very high computing demands, while these methods offer the most suitable way to provide an accurate state of the atmospheric system. The complexity of atmospheric models has been rising with the increase of computational power and scientific knowledge in terms of spatial and temporal resolutions and physical and chemical transport processes. However, it is not enough. To provide a good prediction is also needed to start from a reasonable initial values estimation and reliable emission rates. The provision of a set of optimum parameters can be achieved combining observations with physical and chemical knowledge of atmospheric processes encoded in the numerical models, by space-temporal dimensions variational (4D-Var) data assimilation. The main added value lies on the consistency of the system guaranteed by the inverse simulation of the emitted species and their products. On the other hand, due to the inverse modelling and iterative process enclosed on the 4D-Var data assimilation scheme, the computing time need is, at least, three times longer than a traditional forward run, per iteration (usually 10-20 iterations are needed to minimize the cost function, providing the analysis as close as possible to the observations).
The sophisticated 4D-Var assimilation scheme for gas-phase and aerosols included in the EURopean Air pollution Dispersion – Inverse Model (EURAD-IM), was used to assimilate ground based measurements and satellite retrievals data in order to provide improved initial values and emission factors of gaseous pollutants and aerosol species within the air-shed simulated. The optimal 4D-Var application is the key to quantitatively estimate anthropogenic and biogenic pollutant concentration patterns, as well as to understand their interactions at a given air-shed. The Po-valley region (simulation grid up to 1km of spacial resolution) was defined as a case study due to the existence of measurements by the Zeppelin NT bone instruments on the PEGASOS campaign, during a high concentrations of OH radical episode (July 2012). The add-value from the combination of PEGASOS campaign data with the 4D-Var data assimilation scheme is the provision of improved model results not only at the surface but also in high within the boundary layer. The corrections provided by the observed data to the numerical modelling system are explored, comprehending the highlight of this work, in order to allow the use of these improved results (analysis) for further scientific purposes.

[MET 17] High Resolution Virtual Reality Catchment Simulations for Data Assimilation Experiments

***B. Schalge**, J. Rihani, B. Haese, G. Baroni, D. Erdal, I. Neuweiler, H.J. Hendricks-Franssen, G. Geppert, F. Ament, S. Kollet, O. Cirpka, P. Saavedra, X. Han, S. Attinger, H. Kunstmann, H. Vereecken, C. Simmer*

When simulating hydrological catchments, a high fidelity modeling system is needed. These modeling systems consist of coupled subsurface - land surface – atmosphere (SLAS) models that are able to consider physical processes in each compartment in great detail. In order to make accurate simulations or forecasts, data assimilation (DA) is necessary to get a good initial representation of the system states. However, DA systems currently have not been applied on fully coupled subsurface – land surface – atmosphere models and only to a very

limited extend for models that couple two compartments like subsurface and land surface. Our aim is to develop a new unified DA framework which treats the SLAS in an integrated fashion and avoids compartmentalization of the terrestrial system.
In order to develop such a system, a robust testing environment is needed. For real catchments there are often insufficient measurements available and there is no knowledge about the “true” state of the system to compare the results achieved by DA to.
To alleviate this issue, a high resolution virtual reality (VR) simulation is constructed that serves as a virtual “truth”. Our virtual reality mimics the Neckar catchment in southern Germany. The Neckar catchment was chosen because it features a wide range of topographic features as well as regions of different land use and soil properties. From this VR virtual observations like virtual rain gauges, synoptic stations and satellite observations are extracted. These observations are used to test the new DA framework by comparing fields derived from these observations to the “truth” of the VR.
We use the Terrestrial System Modeling Platform (TerrSysMP), which employs the atmospheric model COSMO, the hydrological model ParFlow and the Community Land Model (CLM3.5) for the land surface coupled by the external coupler OASIS3, to realize the VR simulation.
In the first phase, the VR has to be checked for plausibility. Statistical tests are conducted to evaluate if the VR is within a reasonable margin to what is observed in reality. For that reason, TerrSysMP is run at two different resolutions. To test the atmospheric component, COSMO coupled to CLM is run at a 1.1km resolution over the Neckar catchment for 7 years to get robust statistics of precipitation, the largest water flux in the coupled system. In order to test the hydrologic component ParFlow coupled to CLM is run at a 100m resolution for the upper Neckar subcatchment. These simulations are also valuable to adjust the VR for future simulations to ensure realistic and computationally efficient setups.
For the next phase of the development of the DA system, a fully coupled version of TerrSysMP is run at 1.1km(COSMO)/400m(CLM+ParFlow) resolution to serve as the first version of the VR. Additionally an ensemble of reduced resolution (2.8km/800m) runs is conducted to find the uncertainty sources (vegetation, soil, lateral atmospheric boundaries) which have the largest impact on water and energy fluxes in the terrestrial system. This is an important preparatory step before DA.
With these model runs, evaluation of the different DA components is starting and will be enhanced in the future by upgrading the CLM component to CLM4.5 which allows for resolutions of 100m or even higher for the entire Neckar catchment.

[MET 18] The Global Chemistry Climate Model ECHAM6-HAMMOZ

***M. G. Schultz**, B. Franco, N. Kaffashzadeh, O. Lyapina, S.Schröder, S.Stadtler, O. Stein, D. Taraborrelli, and the international HAMMOZ consortium*

Atmospheric composition of short-lived gases and aerosols is an important component of the global climate system. Complex processes from emissions, transport, and chemical reactions to heterogeneous loss processes and radiation interactions need to be implemented in climate models to reach an adequate understanding of the role of short-lived climate forcers on the climate system and to allow the assessment of climate impacts on the regional scale. With ECHAM6-HAMMOZ we have developed a comprehensive model of tropospheric and stratospheric aerosols and gas-phase chemistry which is now running successfully on the Jülich supercomputer JURECA. We will present an overview of the model architecture, selected evaluation results, and some information about the computational performance of the model as a basis to discuss further science plans.

[MET 19] Molecular Structure of Na(OH) Solutions at High P and T: Insights from *In Situ* Raman Spectroscopy and *Ab Initio* Molecular Dynamics Dimulations

***J. Stefanski**, C. Schmidt, S. Jahn*

Sodium rich peralkaline fluids occur in several processes in the Earth's crust, e.g. late stage hydrothermal reactions in peralkaline agpaitic igneous rocks involve Na(OH) as essential component [1]. Moreover, aqueous Na(OH) solutions at elevated temperature (T) are indispensable in today's chemical industry, e.g. in the aluminum production (Bayer process). Addition of Na(OH) causes substantial changes in the water structure, which are reflected in the Raman spectrum [2] but are not completely understood, particularly at high pressure (P) and temperature.
Here, we investigated structural and vibrational properties of 5.5 and 27 molal sodium hydroxide solutions. The solutions were contained in a hydrothermal diamond anvil cell and analysed by *in situ* Raman spectroscopy from ambient conditions up to 0.8 GPa and 700 °C. *Ab initio* molecular dynamics simulations were used for the interpretation of the spectra. This included Fourier transform of the hydrogen velocity autocorrelation function, *ab initio* Raman spectra [3] and mode-projection approach [4] to decompose normal modes of water and the stretching mode of hydroxide ion.
The simulated frequency spectra agree with the experimentally obtained Raman spectra and show the same changes with P and T. At near ambient conditions, addition of Na(OH) results in rapid destruction of the water network, which confirms earlier studies [5]. At high T, the H3O2 concentration has by far the largest impact on the Raman spectra. The hydrogen bonding distance decreases with increasing P and T because of the proton-transfer between water and the hydroxide ion, which is crucial for Raman spectroscopic analyses using the O—H stretching band as standard. Further observed structural changes with P and T include increasing coordination of Na+ and changes in the connectivity.

[1] Sørensen (1997) Min. Mag. 61, 485-498.
[2] Walrafen, Douglas (2006) J. Chem. Phys. 124, 114504.
[3] Putrino, Parrinello (2002), APS 88, 176401.
[4] Spiekermann et al. (2012), J. Chem. Phys. 136, 154501.
[5] Chen et al. (2002), ACS, 124, 8534-8535.

[MET 20] Terrestrial Systems Numerical Simulations in the Framework of Jülich Research on Exascale Cluster Architectures (JURECA)

***M. Sulis**, P. Shrestha, F. Gasper, K. Kulkarni, K. Goergen, C. Simmer, S. J. Kollet*

Fully coupled, from groundwater to the atmosphere, hydrological models are promising tools for the definition of accurate climate projection, improved weather forecasting, and the identification of sustainable environmental protection and water management strategies. Realizing this potential requires, however, substantial efforts in the development of adequate model physics, and *ad hoc* porting and performance tuning in High-Performance Scientific Computing. This study presents an overview of numerical simulations carried out using a novel integrated hydrological modeling platform (TerrSysMP) in the framework of Juelich Research on Exascale Cluster Architectures (JURECA). The simulations are performed over the North-Rhine Westphalia domain located in western Germany under a range (from diurnal to multi-year) of temporal scales. The overall model response is analyzed (and compared against observations) in terms of root-zone soil moisture dynamics, land surface energy partitioning, and atmospheric forcing (radiation and precipitation).

[MET 21] A Review on Convection Permitting Climate Simulations (CPCS) in the European Alpine Region

***H. Truhetz**, M. Piazza, A. Csáki, L. Herbsthofer, A. F. Prein*

Since their introduction in the late 1980s, regional climate models (RCMs) are widely applied in climate research and climate change impact studies. Nowadays, large ensembles of continent wide climate simulations on the 10 km scale are conducted in internationally coordinated efforts, like the European branch of the Coordinated Downscaling Experiment of the World Climate Research Programme, EURO-CORDEX (www.euro-cordex.net). Thanks to the general progress in computing technology, even higher resolutions became feasible and first so called “convection permitting climate simulations” (CPCSs) with a grid spacing <4 km have emerged.

Within the framework of the projects “Non-Hydrostatic Climate Modelling, Part II” (NHCM-2; www.nhcm-2.eu), funded by the Austrian Science Fund (FWF) (project number P24758-N29), “The Future of Extreme Precipitation Events in the Alpine Region Under High End Climate Change Conditions” (HighEnd:Extremes) (project number KR13AC6K10981) and “Coupled hydrological – climate modelling of floods at small and medium scales in Styria” (CHC-FloodS) (project number KR13AC6K11102), funded by the Austrian Climate Research Programme (ACRP), the still largely unknown potential of CPCSs in the greater Alpine region is investigated. In particular, the models COSMO-CLM and WRF are validated with respect to important synoptic and mesoscale processes and by means of products from Numerical Weather Prediction (NWP) systems with high spatial and temporal resolution (e.g. the nowcasting system INCA of the Austrian Central Institute for Meteorology and Geodynamics and the Swiss forecast system COSMO-7) as well as highly resolved long-term gridded observational dataset.

The poster summarises important results from these projects and introduces new promising developments in the field of process-oriented model validation.

Astrophysics

[A 1] Gravitational Dynamics of Neutron Star Binaries in Numerical Relativity

*B. Brügmann, **M. Bugner**, H. Rüter, T. Dietrich, N. Moldenhauer, D. Hilditch, E. Harms*

Simulations of neutron star binaries in numerical relativity have seen great advances in terms of physical detail and numerical quality. They provide key insight into the general relativistic dynamics and the generation of gravitational waves. We show recent results and inform about the development of new numerical methods.

[A 2] Multidimensional Hydrodynamic Simulations of Stars

*F. Röpke, **P. Edelmann**, A. Bolaños, J. Berberich, L. Horst, F. Lach*

Over the past decades, stellar evolution was modeled under the assumption of spherical symmetry and often in hydrostatic approaches. Dynamical effects were treated in a parametrized form, leading to large uncertainties. With our newly developed code, SLH, we solve the full Euler equations of hydrodynamics in two or three dimensions to study different phases of stellar evolution in detail. As these flows are usually at relatively low Mach numbers ($< 1e^{-2}$), the code employs special discretizations to compute the fluxes accurately. For efficiency it uses implicit time discretization. The iterative linear solvers, which are needed here, are shown to scale quite well to large clusters, like JUQUEEN. We present results from the recent Extreme Scaling workshop. We illustrate the scientific results obtained so far in a study of turbulence properties of our low Mach number solvers and a simulation of turbulent, nuclear combustion in classical novae.

[A 3] Progenitor Systems of Thermonuclear Supernovae

*W. Hillebrandt, **P. Edelmann**, R. Pakmor, K. Marquardt, S. Ohlmann, F. Röpke, M. Kromer*

Type Ia supernovae are believed to result from thermonuclear explosions of white dwarf stars. These events are important for cosmic nucleosynthesis as well as observational cosmology. The stellar systems out of which they emerge and details of their explosion physics, however, remain unclear. The project follows thermonuclear supernova explosions in extensive multidimensional hydrodynamical simulations exploring scenarios that arise from different possible evolutionary channels. In a subsequent step observables are predicted by multidimensional radiation transfer calculations that can then be compared to astronomical data. This facilitates to test whether the considered scenarios are realized in nature. Our approach will be discussed on the example of thermonuclear explosions in hybrid carbon-oxygen-neon white dwarfs.

Computer Science and Numerical Mathematics

[INF 1] Hybrid Parallelism for the DFT Code FLEUR

***U. I. Alekseeva**, D. Wortmann*

Density functional theory (DFT) has transformed material physics and likewise computational chemistry, surface science, nanoscience, and computational biology. This methodology, which provides the capability to describe the electronic structure, interatomic forces and in part also the electronic excitations of molecules and condensed media containing hundreds of atoms in a computational volume, developed into the standard method for realistic description of materials from a quantum mechanical point of view. As it describes the basics of the electronic structure it enables the investigation of the structural, electronic and magnetic properties on atomic length scales.
Modern developments aim at extending the applicability of existing methods by harvesting the power of modern massively parallel computer architectures. We present the current progress of implementing an efficient hybrid parallelization in the code FLEUR, which has been developed by the IAS-1/PGI-1 group in the FZJ. The shared memory OpenMP parallelization augmenting the existing MPI implementation provides not only high one-node performance but also will ensure that current and future supercomputers can be efficiently used to perform large DFT calculations. Besides the discussion of the basic algorithms and their computational challenges, we also demonstrate the improved scalability of the code for realistic example setups.

[INF 2] Scalable Algorithms for Parallel Adaptive Mesh Refinement

*C. Burstedde, J. Fonseca, **J. Holke***

We will display ongoing research in scalable algorithms for parallel adaptive mesh refinement (AMR) at the example of three projects. p4est is a library for AMR on quadrilateral and hexahedral meshes that is being developed since 2007 and scales to more than 1 million MPI processes. We have implemented new shared memory features using MPI 3.1 and will display performance results. t8code is an AMR library for simplicial meshes in development. It implements load-balancing based on our newly developed space-filling curve algorithms for tetrahedra, for which we will show recent experiments. The community code parflow is a parallel watershed flow model developed primarily at LLNL. One goal is to extend parflow to using adaptive meshes via the p4est library, which we have just begun investigating.

[INF 3] FE2TI: Computational Scale Bridging for Dual-Phase Steels

***A. Klawonn**, M. Lanser, O. Rheinbach*

Advanced High Strength Steels (AHSS) provide a good combination of both strength and formability and are therefore applied extensively in the automotive industry, especially in the crash relevant parts of the vehicle. Dual-phase (DP) steel is an example for such AHSS which is widely employed. The excellent macroscopic behavior of this steel is a result of the inherent micro-heterogeneity and complex interactions between the ferritic and martensitic phases in the microstructure. Thus, considering the microscale is indispensable for realistic simulations.
In order to bring large micro-macro simulations to modern supercomputers, we combine the well-known FE^2 scale bridging approach with a highly scalable implementation of the FETI-DP domain decomposition method (Finite Element Tearing and Interconnecting - Dual Primal), which is used as a solver on the microscale. This results in our highly-scalable software

FE2TI. In FE^2, in each Gauss integration point of the macroscopic problem, a microscopic problem is solved on a representative volume element (RVE). The incorporation of the microscale replaces a phenomenological material law on the macroscale. The FE2TI approach is used in the project “EXASTEEL - Bridging scales for multiphase steels” within the the first funding period of the DFG priority program SPP 1648 “Software for Exascale Computing” (SPPEXA). It will be further developed in the second funding period of SPPEXA within the project “EXASTEEL-2: Dual-Phase Steels - From Micro to Macro Properties”. The MPI-parallel C/C++ implementation uses PETSc and efficient solver packages such as BoomerAMG, MUMPS, and UMFPACK are interfaced.
The different RVEs are independent of each other, coupled only through the macroscopic problem and thus can be solved in parallel. In our approach, each RVE is assigned to its own MPI communicator and solved using an inexact-reduced FETI-DP variant. In these highly scalable FETI-DP variants (up to 524K BG/Q cores on Mira, Argonne National Laboratory, USA) the FETI-DP coarse problem is solved inexactly using an AMG (algebraic multigrid) method.
Weak scalability results for different three-dimensional nonlinear, micro-heterogeneous hyperelasticity problems are presented, scaling up to the complete JUQUEEN (458,752 BG/Q cores) at FZ Jülich and the complete Mira ((786,432 BG/Q cores) at Argonne National Laboratory, USA.

[INF 4] Aggregation-Based Multilevel Solvers for Lattice QCD

A. Frommer, K. Kahl, S. Krieg, B. Leder, ***M. Rottmann****, W. Söldner, A. Strebel, K. K. Szabo*

In lattice QCD computations a substantial amount of work is spent in solving discretized versions of the Dirac equation. It has been observed that conventional Krylov solvers show critical slowing down for large lattices and small quark masses. We present a domain decomposition multilevel solver for Wilson-Clover systems and show that considerable speed-up over conventional Krylov subspace methods can be achieved.

[INF 5] Towards Automatic Generation of Energy-Aware Efficient Geometric Multigrid Solvers

C. Schmitt*, S. Kuckuk, S. Kronawitter, A. Grebhahn, H. Rittich*

Many problems in computational science and engineering require the numerical solution of large, sparse linear systems of equations that arise from the discretization of partial differential equations. Multigrid is known to be one of the most efficient methods for this purpose. However, the specific multigrid algorithm and its implementation depend on the underlying problem and hardware.
Project ExaStencils' goal is a compiler and code generation framework capable of generating automatically highly parallel and efficient geometric multigrid solvers. Given an abstract description of the problem, the approach is to choose from a family of options the most suitable composition of variants. We have already been able to showcase a full compilation flow for the investigated class of elliptic partial differential equations for real, as of yet homogeneous, supercomputers such as JUQUEEN.
We provide details of our approach as well as an overview of the different components of our compiler framework.

Scientific Big Data Analysis

[SDBA 1] Deep Learning and Unsupervised Clustering for Analysis of Cellular Cortical Structures in the Human Brain

***C. Bodenstein**, H. Spitzer, P. Glock, M. Riedel, T. Dickscheid*

The Institute INM-1 works on the acquisition of 3D volumetric human brain datasets from post-mortem histological tissue sections. One important image modality is confocal microscopy of cell-stained sections, which allows to study the cytoarchitecture of the brain. Here, image analysis algorithms are used to characterize the density and distribution of cells. While recent work focuses on the mesoscale, with digital image resolutions of down to 20 microns, we are striving towards 3D analysis at subcellular resolution of 1µm. Here, delineations of individual cells become possible, opening the potential to establish new approaches for automated cytoarchitectonic studies. In this project, we focus on the initial problem of segmenting and identifying individual cells in high-resolution image stacks, and on the suitability of supervised deep learning and unsupervised 3D cluster analysis to facilitate the detection of cytoarchitectonic patterns in large, high-resolution datasets. To date we implemented a parallel workflow for cell segmentation with a supervised machine learning component for identifying overlapping cells, which is currently deployed and tested on JURECA. We also performed feasability studies to analyze the potential of convolutional neural networks to distinguish texture patterns in different cortical and subcortical regions of tissue sections, and the potential of clustering algorithms for discovering structure in cell distributions. The latter also included a highly parallel implementation of the DBSCAN algorithm. Ongoing work includes the installation and evaluation of deep learning frameworks and discrete energy minimization algorithms on JURECA.

[SDBA 2] Joint Atmospheric Data Repository and Processing Unit

***S. Grießbach**, L. Hoffmann, O. Stein, K. Görgen, G. Günther, R. Müller, M. Schultz, H. Elbern, C. Hoppe, E. Friese, D. Heinzeller, H. Kunstmann*

Atmospheric science is data intensive science. Atmospheric models may require meteorological input data and chemical boundary conditions that initiate and constrain the simulations. The models also generate output data. Atmospheric science also comprises the analysis of atmospheric data sets, resulting from both measurements and simulations.
A pillar of atmospheric science are reanalysis data sets. Reanalyses contain global 3D information on the atmospheric state, such as temperature, pressure, water vapour content, winds, and chemical composition. They are widely used as initial and lateral boundary conditions for atmospheric simulations, as initial conditions for satellite data retrievals and are itself subject to extensive data analyses.
With respect to observational data sets, the latest generation of satellite instruments provides large data sets (10 TB+ each) of global measurements. An essential part of the work with satellite data in Jülich is the processing of the measurement data. Yet, at the moment a large fraction of the processing time is spent on waiting for the data to be copied from the band archive to the work file system. Having several different data sets readily available for processing will allow new types of scientific studies to be conducted.
The atmospheric research groups would greatly benefit from a fast, easily accessible and properly dimensioned atmospheric data storage, processing and sharing infrastructure at JSC. The productivity enhancing advantages of the advanced atmospheric data infrastructure are:

- reduction of data transfer to and from JSC
- reduction of required archive space (data is archived only once)

- reduction of data archive maintenance work (e.g. as a service of SimLab Climate to community)
- high availability to support operational tasks
- closer collaboration between the groups and homogenization of data formats

Starting our project, we focused on the reanalyses of the European Centre for Medium-Range Weather Forecasts (ECMWF) (ERA-interim) that are extensively used in Jülich. Common practice at the moment is that each group transfers, pre-processes, and archives the reanalysis data. For ERA-interim this are about 30 TB per group. However, the next generation of reanalyses will comprise 240 TB. This rapid increase is a challenge for the data storage resources of each group as well as for data handling on the supercomputers. Due to the large data overlap between the groups and the data size challenges of future reanalyses, we started to compile and test a reanalysis data archive that can be accessed by all partners on the Jülich supercomputers as well as from the workstation clusters within Forschungszentrum Jülich.
The 'Joint atmospheric data repository and processing unit' will allow a substantial step forward to a combined use of data and the application of a new generation of meteorological data sets, which is critical for the scientific success of the participating institutes.

[SDBA 3] Turbulence Database from Direct Numerical Simulations

***J. H. Göbbert**, M. Gauding, B. Tweddell*

The motion of turbulent flows is one the unsolved problems of classical physics and is of both fundamental and practical importance. Turbulent flows exhibits many anomalies that are not well understood and of interest for a large research community. Due to this complexity turbulent flows are difficult to attack by rigorous analytic theories. In turbulence unknown statistical quantities emerge for which no governing equation exists.
A solution of turbulent flows can be obtained by numerical methods. Direct numerical simulation (DNS) solves the governing equations. It does not relay on turbulence models, since all relevant scales are numerically resolved. DNS allows to simulate turbulent flows at sufficiently high Reynolds numbers with at the same time high resolution of the fine-scales. For high Reynolds number flows it is customary to solve the Navier-Stokes equation in a periodic box by means of a pseudo-spectral approach.
Over the past years DNS of turbulent flows has been conducted at the supercomputer JUQUEEN. The present simulations belong to the most comprehensive work of its kind and are unique in the sense that the small scales are resolved with a higher accuracy compared to that reported in literature. Motivated by the obtained results new questions arise so that a continuously analysis of the data can be possible.
With the development of a data sharing concept of a highly resolved DNS results based on a turbulence database our principal intention is to simplify the access and further post-processing by different research groups world-wide.

[SDBA 4] Implementation of Parallel NetCDF in the ParFlow Hydrological Model: A Code Modernisation Effort as Part of a Big Data Handling Strategy

***L. Poorthuis**, K. Goergen, W. Sharples, S.Kollet*

State-of-the-art geoscience simulations are tending towards ever increasing model complexity. This is due to the incorporation of multi-physics and fully coupled model systems, often in combination with higher spatial resolutions. In addition, simulations are being run for longer time periods in order to model phenomena such as climate change and water resources. These factors combined lead to a big data challenge. This data challenge is

typically characterized by the TB-scale data volumes involved, namely I/O, where data variety, velocity and complexity are smaller issues in comparison. In this context, the NIC Scientific Big Data Analytics project “Towards a high-performance big data storage, handling and analysis framework for Earth science simulations” has been working since autumn 2015 on a code modernisation effort, towards a big data readiness of geoscience simulation codes, and data processing and analysis applications. The simulation code considered is the massively MPI-parallel hydrological model ParFlow. Thus far, work has centred around the modernisation of ParFlow's parallel I/O: A standalone C code was used to assess and test the pNetCDF and the HDF5-based NetCDF4 I/O libraries' features and their parallel read and write performance. Tuning and scaling studies on the JSC/JURECA HPC system led to optimised runtime environment settings and a near linear scaling behaviour of the API. This MPI C-code can be used as a showcase implementation for parallel I/O for some of the Geoverbund ABC/J modelling groups. The NetCDF4 interface was chosen as it constitutes a quasi-standard in geosciences and ensures consistent and efficient data flow paths and compression. The I/O testing and the scaling experiments have been done in a JUBE2-based benchmarking framework which also integrates the Score-P profiling and tracing infrastructure, the Scalasca performance optimisation tool and the Darshan HPC I/O characterisation tool. This JUBE2-based framework was then further extended to act as a portable generic testing platform for all benchmarking, development and testing work with ParFlow, including idealised and real data reference test cases for weak and strong scaling studies, a variety of compiler options, as well as common profiling tools, which are all embedded in an easy to use run environment. To further improve ParFlow's I/O functionality, we propose adding NetCDF4 interfaces that write to a shared compressed NetCDF file concurrently with one MPI task per node. The proposed code will automatically adjust for the computational set up, such as gathering of data on single node, number of nodes, I/O interfaces and MPI ranks per node. Another obvious big data challenge for complex geoscience simulations is post-processing terabytes of data. Therefore we plan to develop on-the-fly processing and visualisation for ParFlow, once the I/O optimisation is finished. This will be a joint effort with the JSC Cross Sectional Team Visualisation, in order to implement an *in situ*, i.e. during runtime, processing and visualisation functionality, using the VisIt software. Additionally, this will help to improve scalability and performance whilst substantially reducing total processing time and model output.

[SDBA 5] Statistical Analysis of High-Rayleigh Number Turbulent Convection Data

A. Pandey, A. Kolchinskaya, J. D. Scheel, ***J. Schumacher***

We consider high-Rayleigh number convection in a closed cylindrical cell. In the present scientific big data analysis proposal we would like to address the following scientific questions:

1. Can we remove the large-scale circulation (LSC) flow in the closed convection cell by a Proper Orthogonal Decomposition (POD) analysis more efficiently such that a transition from Gaussian to non-Gaussian statistics of velocity derivatives can be revealed?
2. How does the structure and strength of the LSC vary with Prandtl number at a given Rayleigh number?
3. What is the form of the energy spectra in the bulk of the cell; is it Kolmogorov-like as in homogeneous isotropic turbulence?
4. Which scaling is obtained for the energy and thermal dissipation rates as a function of Rayleigh and Prandtl number?
5. How do the velocity gradients at the wall affect the generation of plumes in low-Prandtl number convection?

[SDBA 6] Mining Peptide Aggregation Patterns in Atomistic Monte Carlo Simulations

*Y. Lu, **O. Zimmermann**, S. Mohanty, T. Seidl*

Monte Carlo methods provide an efficient alternative to Molecular Dynamics for the atomistic simulation of biological processes that operate on large time scales such as protein folding and peptide aggregation.
The high dimensionality and the vast number of conformations from Monte Carlo simulations pose serious problems to data analysis. To gain further insight into the details of structure formation processes from these simulations we have developed a prototype of an analysis framework to enable efficient mining of peptide and protein structure ensembles. Preliminary analysis of a large scale peptide aggregation simulation is used to demonstrate the utility of the framework.

Participants

Name	First name	Institution	Poster
Abad	Enrique	German Research School for Simulation Sciences	BIO 9
Abaurrea	Clara	Forschungszentrum Jülich, ICS-2/IAS-2	BIO 10
Albe	Karsten	TU Darmstadt	
Alekseeva	Uliana	Forschungszentrum Jülich, PGI-1/IAS-1	INF 1
Alleva	Claudia	Forschungszentrum Jülich, ICS-4	BIO 11
Anders	Frithjof	TU Dortmund	
Arnold	Lukas	Forschungszentrum Jülich, JSC	ST 1
Aschikhin	Alexander	DESY Hamburg	PLA 1
Banerjee	Debasish	DESY Zeuthen	E 1
Barragan-Yani	Daniel	TU Darmstadt	MAT 1
Behbahani	Mehdi	Aachen University of Applied Sciences	ST 2
Bergner	Georg	University of Bern	E 2
Berndt	Jonas	Forschungszentrum Jülich, IEK-8	MET 1
Biermann	Peter L.	MPI für Radioastronomie	
Binder	Kurt	Johannes Gutenberg Universität Mainz	
Bittkau	Karsten	Forschungszentrum Jülich, IEK-5	KM 1
Bochicchio	Anna	GRS and Forschungszentrum Jülich, IAS-5/INM-9	BIO 7
Bode	Mathis	RWTH Aachen	ST 3
Bodenstein	Christian	Forschungszentrum Jülich, JSC	SBDA 1
Boeck	Thomas	TU Ilmenau	ST 4
Bonus	Michele	Heinrich Heine Universität Düsseldorf	BIO 12
Bourdick	Axel	Universität Bayreuth	BIO 13
Brockmann	Jan Martin	University of Bonn	MET 2
Bruckmann	Johanna	RWTH Aachen	MET 3
Bugner	Marcus	University of Jena	A 1
Böckmann	Marcus	Westfälische Wilhelms-Universität Münster	MAT 2
Bücker	Oliver	Forschungszentrum Jülich, JSC	BIO 8
Cakircali	Metin	Forschungszentrum Jülich and RWTH Aachen	ST 9
Calandrini	Vania	Forschungszentrum Jülich, IAS-5/INM-9	
Caldeira	Liliana	Forschungszentrum Jülich, INM-4	
Cao	Ruyin	Forschungszentrum Jülich, IAS-5	BIO 14
Casasnovas Perera	Rodrigo	Forschungszentrum Jülich, IAS-5	BIO 15
Ciupka	Daniel B.	Heinrich Heine Universität Düsseldorf	BIO 16
Coto	Pedro B.	FAU Erlangen-Nürnberg	
Czaja	Philippe	Forschungszentrum Jülich, IEK-5	MAT 3
Dang	Siaufung	Forschungszentrum Jülich, IEK-2	MAT 4
Dapp	Wolf	Forschungszentrum Jülich, JSC	
De Raedt	Hans	University of Groningen	
Diesmann	Markus	Forschungszentrum Jülich, INM-6	
Dornmair	Irene	Universität Hamburg / CFEL	PLA 2
Drzycimski	Kevin	Forschungszentrum Jülich, JSC	

Name	First name	Institution	Poster
Dąbrowski	Jarek	Innovations for High Performance Microelectronics	MAT 5
Edelmann	Philipp	Heidelberg Institute for Theoretical Studies	A 2, A 3
Eisenstecken	Thomas	Forschungszentrum Jülich, IAS-2	BIO17
Elbern	Hendrik	Forschungszentrum Jülich und Universität Köln	
Ermes	Markus	Forschungszentrum Jülich, IEK-5	
Fierro	Fabrizio	German Research School for Simulation Sciences	BIO 25
Franke	Philipp	Forschungszentrum Jülich, IEK-8	MET 4
Frieg	Benedikt	Heinrich Heine Universität Düsseldorf	BIO 4
Froning	Dieter	Forschungszentrum Jülich, IEK-3	ST 5
Gauding	Michael	TU Freiberg	ST 6
Gerstner	Philipp	Heidelberg University	MET 5
Gibbon	Paul	Forschungszentrum Jülich, JSC	
Giudice	Pietro	Westfälische Wilhelms-Universität Münster	E 3
Glock	Philipp	Forschungszentrum Jülich, INM-1	
Gohlke	Holger	Heinrich-Heine-Universität Düsseldorf	
Grauer	Rainer	Ruhr-University Bochum	
Grießbach	Sabine	Forschungszentrum Jülich, JSC	SBDA 2
Grotendorst	Johannes	Forschungszentrum Jülich, JSC	
Grynko	Yevgen	University of Paderborn	PLA 3
Göbbert	Jens Henrik	Forschungszentrum Jülich, JSC	SBDA 3
Görgen	Klaus	Forschungszentrum Jülich, JSC	
Götzfried	Paul	TU Ilmenau	ST 7
Götz	Markus	Forschungszentrum Jülich, JSC	
Haas	Sarah	Forschungszentrum Jülich, INM-1	
Hahne	Jan	Bergische Universität Wuppertal	BIO 2
Henry	Ewan	Forschungszentrum Jülich, ICS-2	BIO 18
Hesselmann	Stephan	RWTH Aachen	KM 2
Hlushkou	Dzmitry	Philipps-Universität Marburg	MAT 6
Hoefler-Thierfeldt	Sabine	Forschungszentrum Jülich, JSC	
Hoeft	Matthias	Thüringer Landessternwarte Tautenburg	
Hoelbling	Christian	Wuppertal University	E 4
Hofmeister	Richard	Helmholtz-Zentrum Geesthacht	MET 6
Holke	Johannes	University of Bonn	INF 2
Hoore	Masoud	Forschungszentrum Jülich, ICS and IAS	BIO 19
Hoppe	Charlotte	Forschungszentrum Jülich, IEK-8	
Hsu	Hsiao-Ping	Max Planck Institute for Polymer Research	POLY 1
Huang	May	Forschungszentrum Jülich, INM9	BIO 20
Huynh	Anh-Minh	Forschungszentrum Jülich, INM-1	
Huysegoms	Marcel	Forschungszentrum Jülich, INM-1	
Hüter	Claas	Forschungszentrum Jülich, IEK-2	
Ippoliti	Emiliano	Forschungszentrum Jülich, IAS-5/INM-9	
Jacob	Daniela	Climate Service Center Germany (GERICS)	MET 7
Jahn	Sandro	University of Cologne	MET 8
Jalkanen	Jari	Forschungszentrum Jülich, JSC	

Name	First name	Institution	Poster
Jana	Richard	Karlsruhe Institute of Technology	MAT 7
Janetzko	Florian	Forschungszentrum Jülich, JSC	
Janke	Wolfhard	Universität Leipzig	KM 3
Jin	Fengping	Forschungszentrum Jülich, JSC	KM 4
Ji	Yaqi	Forschungszentrum Jülich, IEK-6	MAT 8
Jones	Robert	Forschungszentrum Jülich, PGI-1	
Junnarkar	Parikshit	Helmholtz Institut Mainz	E 5
Kaffashzadeh	Najmeh	Forschungszentrum Jülich, IEK-8	
Karbach	Carsten	Forschungszentrum Jülich, JSC	
Karhan	Kristof	Universität Paderborn	CH 1
Kasradze	Ketevan	University of Cologne	MET 9
Kerroumi	Iman	FH Aachen	
Klawonn	Axel	Universität zu Köln	INF 3
Knechtli	Francesco	University of Wuppertal	E 6
Kollet	Stefan	Forschungszentrum Jülich, IBG-3	MET 10
Kremer	Manfred	Forschungszentrum Jülich, JSC	
Kulikovsky	Andrei	Forschungszentrum Jülich, IEK-3	
Kurtz	Wolfgang	Forschungszentrum Jülich, IBG-3	MET 11
Kurzmann	André	Karlsruhe Institute of Technology	MET 12
Kämpfer	Julia	Forschungszentrum Jülich, JSC	
Köhnen	Stefan	Forschungszentrum Jülich, INM-1	
Körfgen	Bernd	Forschungszentrum Jülich, JSC	
Köstler	Harald	FAU Erlangen-Nürnberg	
Kühbach	Markus T.	RWTH Aachen	
Laermann	Edwin	Universität Bielefeld	
Lanser	Martin	Universität zu Köln	
Lehmann	Götz	Heinrich-Heine-Universität Düsseldorf	
Leroy	Frédéric	TU Darmstadt	
Lippert	Thomas	Forschungszentrum Jülich, JSC	
Liseykina	Tatyana	Universität Rostock	PLA 4, PLA 5
Machtens	Jan-Philipp	Forschungszentrum Jülich, ICS-4	
Marinova	Valeriia	FH Aachen	
Mehrabian	Hadi	University of Twente	POLY 2
Meinke	Jan	Forschungszentrum Jülich, JSC	
Mellado	Juan P.	Max Planck Institute for Meteorology	MET 13
Memon	Shahbaz	Forschungszentrum Jülich, JSC	
Menzel	Miriam	Forschungszentrum Jülich, INM-1	BIO 3
Meyer	Kai-Christian	TU Darmstadt	MAT 9
Michielsen	Kristel	Forschungszentrum Jülich, JSC	
Mießen	Christian	RWTH Aachen	
Mohlberg	Hartmut	Forschungszentrum Jülich, INM-1	BIO 5
Müller	Marcus	Georg-August Universität Göttingen	POLY 3
Müser	Martin	Forschungszentrum Jülich, JSC	MAT 10

Name	First name	Institution	Poster
Nielaba	Peter	University of Konstanz	
Orth	Boris	Forschungszentrum Jülich, JSC	
Pagani	Giulia	Heinrich-Heine-Universität Düsseldorf	BIO 21
Pavlin	Matic	German Research School for Simulation Sciences	BIO 1
Perlt	Holger	Universität Leipzig	E 7
Pesce	Luca	Forschungszentrum Jülich, IAS-5 and INM-9	BIO 22
Pietrzyk	Uwe	Forschungszentrum Jülich, INM-4	
Pinke	Christopher	Goethe-Universität Frankfurt	E 10
Poorthuis	Lukas	Forschungszentrum Jülich, JSC	SBDA 4
Popescu	Voicu	University Duisburg-Essen	MAT 11
Popov	Anton	Johannes Gutenberg Universität Mainz	MET 14
Poulsen	Mads Bruun	University of Copenhagen	MET 15
Qi	Shuanhu	Johannes Gutenberg Universität Mainz	POLY 4
Renze	Peter	Hochschule Ulm	
Reuber	Georg	Johannes-Gutenberg Universität Mainz	
Rheinbach	Oliver	TU Bergakademie Freiberg	
Ribeiro	Isabel	Universität zu Köln	MET 16
Riedel	Morris	Forschungszentrum Jülich, JSC	
Rivas	Nicolas	Helmholtz Institute Erlangen Nuremberg	POLY 6
Rohlfing	Michael	Westfälische Wilhelms-Universität Münster	KM 5
Romero	Pedro A.	Fraunhofer IWM	
Rossetti	Giulia	Forschungszentrum Jülich and RWTH UKA	
Rottmann	Matthias	Bergische Universität Wuppertal	INF 4
Sandal	Massimo	Forschungszentrum Jülich, INM-9/IAS-5	BIO 23
Schalge	Bernd	University of Bonn	MET 17
Scheurer	Christoph	TU München	MAT 12
Schmitt	Christian	FAU Erlangen-Nürnberg	INF 5
Schnurpfeil	Alexander	Forschungszentrum Jülich, JSC	
Schober	Martin	Forschungszentrum Jülich, INM-1	
Schröder	Sabine	Forschungszentrum Jülich, IEK-8	
Schultz	Martin	Forschungszentrum Jülich, IEK-8	MET 18
Schumacher	Jörg	TU Ilmenau	ST 8, SBDA 5
Schwenk	Achim	TU Darmstadt	
Seifried	Daniel	Universität zu Köln	
Spatschek	Robert	Forschungszentrum Jülich, IEK-2	MAT 13
Spitzer	Hannah	Forschungszentrum Jülich, INM-1	
Stefanski	Johannes	Universität zu Köln	MET 19
Stockem Novo	Anne	Ruhr-University Bochum	PLA 6
Strebel	Artur	Bergische Universität Wuppertal	E 8
Strodel	Birgit	Forschungszentrum Jülich, ICS-6	BIO 24
Sukhomlinov	Sergey	Forschungszentrum Jülich, JSC	
Sulis	Mauro	University of Bonn	MET 20
Syranidis	Konstantinos	Forschungszentrum Jülich, IEK-3	

Name	First name	Institution	Poster
Szabo	Kalman	Forschungszentrum Jülich, JSC	E 9
Taraborrelli	Domenico	Forschungszentrum Jülich, IEK-8	
Toth	Balint	University of Wuppertal	
Trebst	Simon	University of Cologne	KM 6
Truhetz	Heimo	University of Graz	MET 21
Veluswamy	Krishnaswamy	RWTH Aachen	
Vidossich	Pietro	German Research School for Simulation Sciences	BIO 6
von Mach	Christian	Forschungszentrum Jülich, IBG-3	
Walter	Johannes	FAU Erlangen-Nürnberg	SE 1
Weng	Chi-Hung	University of Freiburg	AK 1
Wenschuh	Ulrich	Deutsche Post AG	
Wiebeler	Hendrik	Universität Paderborn	CH 2
Zeller	Rudolf	Forschungszentrum Jülich, IAS-3	MAT 14
Ziaei	Vafa	Mulliken Center for Theoretical Chemistry	CH 3
Zierenberg	Johannes	Universität Leipzig	POLY 5
Zimmermann	Olav	Forschungszentrum Jülich, JSC	SBDA 6
Zirwes	Thorsten	Karlsruhe Institute of Technology	CH 4